

73-1250

LIBRARY

FEB 25 1974

Lunar Science Institute

LUNAR THERMAL MEASUREMENTS IN CONJUNCTION WITH
PROJECT APOLLO

by

Sydney P. Clark, Jr.

Final Report

September 1973

Grant No. NGR-07-004-039

Yale University

New Haven, Connecticut 06520

LIBRARY
LUNAR SCIENCE INSTITUTE
HOUSTON, TEXAS 77058

The information presented herein was developed from NASA-funded work. Since the report preparation was not under NASA control, all responsibility for the material in this document must necessarily reside in the author.

NATIONAL AERONAUTICS AND SPACE ADMINISTRATION

N 74-10769
NASA CR-13603

This grant funded feasibility studies and development work on the lunar heat flow experiment (HFE). The first task was performed under a previous grant (NSG-400), and it consisted, among other things, of the investigation of a novel method of measuring heat flow which has the advantage of not requiring a drilled hole. The method was found not to be feasible, however, and the requirement that a drill be developed for lunar use was established. These early results are incorporated in Appendix I for convenience.

Once the necessity of drilling a hole in the moon became clear, it became desirable to develop an in situ method of measuring lunar thermal conductivity. The alternative, to measure conductivity on a returned core, suffers from the disadvantages that the volume available for investigation is much smaller than that sampled by the in situ method and the physical properties of the lunar material may be permanently altered by the coring operation. The temperature field surrounding a heater with the geometry of a cylinder of finite length was therefore investigated. The results were presented in an interim report dated January, 1967 (Appendix II). The calculations reported there formed the basis of the design of the downhole part of the HFE, which was developed and fabricated by A. D. Little, Inc.

During the final six years of the grant's duration the main activity was travel and consultation with colleagues associated with planning and fabricating the HFE. Places most frequently visited were Lamont-Doherty Geological Observatory and A. D. Little, Inc.

Probably the best measure of the success of a research program is its results. Four HFE's have been flown and two of these are in place on the

moon and returning data of high quality. They have achieved and even surpassed their design objectives, and they have proven themselves to be rugged, reliable instruments. They are described in the Apollo 15 and Apollo 17 Preliminary Science Reports, attached as Appendix III. The two instruments that failed to return data were victimized by circumstances that were unrelated to the HFE itself. One was lost as a consequence of the abort of the Apollo 13 landing. On the Apollo 16 mission, the HFE was successfully emplaced, but it was silenced when an astronaut inadvertently tripped and broke the cable connecting it to ALSEP.

APPENDIX I

Some Early Feasibility Studies

**SOME CALCULATIONS PERTAINING TO THE FEASIBILITY OF
MEASURING LUNAR HEAT FLOW**

by Sydney P. Clark, Jr.

Final Report

September 1965

Prepared under Contract No. NsG-400

**Yale University
New Haven, Connecticut**

The information presented herein was developed from NASA-funded work. Since the report preparation was not under NASA control, all responsibility for the material in this document must necessarily reside in the author.

NATIONAL AERONAUTICS AND SPACE ADMINISTRATION

Contents

	Page
Introduction	1
Steady periodic temperatures in a 3-layered medium	4
Steady periodic temperatures near a hole in the surface layer	16
Steady-state perturbations of flux due to irregularities in the thickness of the surface layer	18
The blanket method of measuring lunar heat flow	21
Conclusions	29
Acknowledgments	32
References cited	33

Illustrations

	Following page
1a, b, c	14
2	14
3a, b	14
4a, b	14
5	14
6	14
7	17
8	19
9	23
10	26

ABSTRACT

A number of problems related to the feasibility of measuring lunar heat flow at the lunar surface or in a shallow hole have been investigated with the following results. Study of the steady periodic temperatures in the lunar material will give unambiguous information about its properties only if the surface material alone has an appreciable effect on the amplitude and phase of the thermal wave. Layering tends to reduce the amplitude of the fluctuation at a given depth. High-amplitude fluctuations near a place where the poorly conducting surface layer is missing do not penetrate far and pose no difficulty. Large perturbations of heat flow may be caused by irregularities in thickness of the surface layer, and a number of closely spaced measurements at a given landing site will be required to minimize this source of error. The "blanket" method of measuring lunar heat flow is not considered feasible because of the necessity of very closely matching the local albedo with the blanket, and because a blanket with properties such that an easily measured gradient free from periodic fluctuations can be set up by the lunar flux requires a prohibitively long time to come to thermal equilibrium. Conversely a blanket with a suitable time constant will yield only a small, seriously disturbed gradient that will be difficult to measure.

1. INTRODUCTION

A measurement of lunar heat flow will be interesting for a number of scientific reasons. Heat flow gives more direct evidence about the internal thermal regime of a planet than any other measurement that can be made at the surface. Limits to the total amount of radioactive elements in the planet's interior can be set, as well as limits to its initial temperature. In the case of the moon, a determination of heat flow will help to decide just how "dead" it is, since the source of volcanism and mountain building must ultimately be thermal energy, most of which is leaked to the surface to appear as heat flow. The small size of the moon makes it especially interesting from the thermal point of view. Cooling from the surface has affected some 70% of the volume of the moon compared with about 20% of the earth, assuming the two bodies are of the same age. As a consequence the relative importance of initial heat and radiogenic heat may be very different on the moon as compared with the earth, a possibility which makes a comparison of heat flow from the two bodies all the more interesting.

But granting the desirability of a measurement of lunar heat flow, a number of obstacles remain in the way. On the terrestrial land surface heat flow is measured in boreholes, mines or tunnels reaching depths up to several thousand feet. Considerable depths are necessary in order to avoid disturbances which occur near the surface. There is no prospect of drilling a deep hole in the moon in the foreseeable future, and any measurement of heat flow must be made at the surface or in a shallow hole. The temperatures near the lunar surface are in the first place affected by the large monthly variation in surface temperature, and secondly by

thermal refraction due to variability in the thickness of the lunar surface material, which is known to be of very low thermal conductivity compared to solid rock. The goal of the present study is to assess the seriousness of these difficulties.

In the calculations which follow, the assumption that the lunar situation can be adequately represented by a linear model, i.e. a model in which the thermal properties of the lunar material are treated as independent of temperature, is made. This assumption is probably very wrong for materials near the lunar surface under ambient lunar conditions. Temperatures are below the Debye temperatures of common rock-forming minerals, implying a temperature-dependent specific heat. Radiative transfer is presumably an important contributor to the thermal conductivity of the porous surface material, and it is strongly dependent on temperature. Both factors argue for treatment of nonlinear models, but the additional complication is hardly warranted in view of the remaining uncertainties in the details of the properties of the lunar surface material. Thus the present study represents a first approach to the problem, aimed more at recognizing difficulties than at removing them.

Four problems are considered in detail in the following sections. The first is the case of one-dimensional steady periodic heat flow in a stratified medium consisting of two layers of differing thermal properties, resting on a substratum of infinite thickness which has a third set of thermal constants. An exact solution is obtained for the case of semisoidally varying surface temperature.

A second problem again concerns steady periodic temperatures, this time in a two-layered medium with the upper layer absent within a circular

region. Numerical results are obtained for this model of a hole in the moon's poorly conducting surface layer. Perturbations of heat flow due to variable thickness of the surface layer are investigated under steady-state conditions, and finally results are extended to calculations of the disturbances associated with the emplacement of a blanket-type thermal fluxmeter on the lunar surface.

2. STEADY PERIODIC TEMPERATURES IN A 3-LAYERED MEDIUM

A. Theory

Mathematically the problem can be expressed in the following way. The region $0 \leq x \leq X_1$ contains material with properties K_1 , ρ_1 , c_1 , etc. (see table 1 for notation), the region $X_1 \leq x \leq X_3$ contains material with properties K_2 , etc., and the region $x \geq X_3$ contains material with properties K_3 , etc. At the boundaries X_1 and X_3 both temperature and thermal flux ($= K \frac{\partial T}{\partial x}$) are continuous, $T \rightarrow 0$ as $x \rightarrow \infty$, and $T = A_0 \sin \omega t$

when $x = 0$, where A_0 is the constant surface amplitude. Within each region T must satisfy the equation of heat conduction, $\frac{\partial^2 T}{\partial x^2} = \frac{1}{\alpha} \frac{\partial T}{\partial t}$

This problem is most conveniently solved by the Laplace transform method described by Carslaw and Jaeger (1959). Further details about this particular problem are given by Lachenbruch (1959), who obtained the solution for the special case $x = X_3$. If we write \bar{T} for the Laplace transform of T , and use subscripts to identify the three regions, we have (Lachenbruch, 1959):

$$\bar{T}_1 = F \exp(q_1 x) + G \exp(-q_1 x), \quad (1)$$

$$\bar{T}_2 = H \exp(q_2 x) + J \exp(-q_2 x), \quad (2)$$

$$\bar{T}_3 = R \exp(-q_3 x), \quad (3)$$

where F , G , H , J , and R are constants, independent of x . The two boundary conditions at each interface, $x = X_1$ and $x = X_3$, plus the condition at $x = 0$, provide 5 equations which determine the 5 unknown quantities F , G , H , J , and R .

Table 1. Definitions of Symbols

T	Temperature
t	Time
x	Depth variable
X_1	Depth to base of upper layer
X_2	Depth beneath base of upper layer
X_3	Depth to top of substratum, $=X_1 + X_2$
ω	Angular frequency, $= 2.66 \times 10^{-6} \text{ sec}^{-1}$ for 1 lunar day
K_i	Thermal conductivity of the ith layer
ρ_i	Density of the ith layer
c_i	Heat capacity of the ith layer
α_i	Thermal diffusivity of the ith layer, $= K_i / \rho_i c_i$
β_i	Thermal inertia of the ith layer, $= (K_i \rho_i c_i)^{1/2}$
p	Parameter of the Laplace Transform, $\bar{T} = \int_0^\infty \exp(-pt) T dt$
q_i	$(p/\alpha_i)^{1/2}$
Q	Heat flow
L	Thickness of blanket
b	Subscript denoting properties of blanket

We find

$$F = \frac{A_0 \omega \exp(-q_3 X_3 - q_1 X_1)}{(p^2 + \omega^2) \Delta} [(-\beta_2 \beta_3 - \beta_1 \beta_3 + \beta_2^2 + \beta_2 \beta_1) \exp(-q_2 X_2) + (-\beta_2 \beta_3 + \beta_1 \beta_3 - \beta_2^2 + \beta_2 \beta_1) \exp(q_2 X_2)] \quad (4)$$

$$G = \frac{A_0 \omega \exp(q_1 X_1 - q_3 X_3)}{(p^2 + \omega^2) \Delta} [(-\beta_2 \beta_3 + \beta_1 \beta_3 + \beta_2^2 - \beta_1 \beta_2) \exp(-q_2 X_2) + (-\beta_2 \beta_3 - \beta_1 \beta_3 - \beta_2^2 - \beta_1 \beta_2) \exp(q_2 X_2)] \quad (5)$$

$$H = \frac{2A_0 \omega \exp(-q_2 X_3 - q_3 X_3)}{(p^2 + \omega^2) \Delta} (\beta_1 \beta_2 - \beta_1 \beta_3) \quad (6)$$

$$J = \frac{2A_0 \omega \exp(q_2 X_3 - q_3 X_3)}{(p^2 + \omega^2) \Delta} (\beta_1 \beta_2 + \beta_1 \beta_3) \quad (7)$$

$$R = \frac{A_0 \omega \exp(-q_1 X_1 - q_2 X_2 + q_3 X_3)}{(p^2 + \omega^2) \Delta} (4\beta_1 \beta_2), \quad (8)$$

where

$$\begin{aligned} \Delta = & (-\beta_2 \beta_3 - \beta_1 \beta_3 + \beta_2^2 + \beta_2 \beta_1) \exp(-2q_2 X_2 - 2q_1 X_1) + \\ & + (-\beta_2 \beta_3 + \beta_1 \beta_3 - \beta_2^2 + \beta_2 \beta_1) \exp(-2q_1 X_1) + \\ & + (\beta_2 \beta_3 - \beta_1 \beta_3 - \beta_2^2 + \beta_2 \beta_1) \exp(-2q_2 X_2) + \\ & + (\beta_2 \beta_3 + \beta_1 \beta_3 + \beta_2^2 + \beta_2 \beta_1) \end{aligned} \quad (9)$$

and $X_2 = X_3 - X_1$.

The transforms of equations (1)-(3) can be inverted by the contour integration method. Lachenbruch (1959) has already shown that the line integrals involved in the inversion contribute only to the initial transient state and have nothing to do with steady periodic temperatures. Hence for present purposes we need consider only the residues at the poles of the transforms. Poles are located at $p = \pm i\omega$; following Lachenbruch, we assume that the quantity Δ (equation 9) has no zeros in the complex plane. It can be shown that the solution given below does indeed satisfy all of the conditions of the problem, which constitutes proof that either Δ has no zeros or that the residues at the resulting poles contribute nothing to the steady periodic part of the solution.

The residues at $p = \pm i\omega$ lead to the following expressions for the temperatures.

$$\begin{aligned}
 T_1 = & \frac{A_0}{D} \{ \exp(-\sqrt{\omega/2\alpha_1}x) \sin(\omega t - \sqrt{\omega/2\alpha_1}x) + \\
 & + P_2 [\exp(-2\sqrt{\omega/2\alpha_1}X_1 - 2\sqrt{\omega/2\alpha_2}X_2 + \sqrt{\omega/2\alpha_1}x) \sin(\omega t - 2\sqrt{\omega/2\alpha_1}X_1 - 2\sqrt{\omega/2\alpha_2}X_2 + \sqrt{\omega/2\alpha_1}x) + \\
 & + \exp(-2\sqrt{\omega/2\alpha_1}X_1 - 2\sqrt{\omega/2\alpha_2}X_2 - \sqrt{\omega/2\alpha_1}x) \sin(\omega t + 2\sqrt{\omega/2\alpha_1}X_1 + 2\sqrt{\omega/2\alpha_2}X_2 - \sqrt{\omega/2\alpha_1}x)] + \\
 & + P_3 [\exp(-2\sqrt{\omega/2\alpha_1}X_1 + \sqrt{\omega/2\alpha_1}x) \sin(\omega t - 2\sqrt{\omega/2\alpha_1}X_1 + \sqrt{\omega/2\alpha_1}x) + \\
 & + \exp(-2\sqrt{\omega/2\alpha_1}X_1 - \sqrt{\omega/2\alpha_1}x) \sin(\omega t + 2\sqrt{\omega/2\alpha_1}X_1 - \sqrt{\omega/2\alpha_1}x)] + \\
 & + P_4 [\exp(-2\sqrt{\omega/2\alpha_2}X_2 - \sqrt{\omega/2\alpha_1}x) \sin(\omega t - 2\sqrt{\omega/2\alpha_2}X_2 - \sqrt{\omega/2\alpha_1}x) + \\
 & + \exp(-2\sqrt{\omega/2\alpha_2}X_2 - \sqrt{\omega/2\alpha_1}x) \sin(\omega t + 2\sqrt{\omega/2\alpha_2}X_2 - \sqrt{\omega/2\alpha_1}x)] + \\
 & + P_2 P_3 [\exp(-4\sqrt{\omega/2\alpha_1}X_1 - 2\sqrt{\omega/2\alpha_2}X_2 + \sqrt{\omega/2\alpha_1}x) \sin(\omega t + 2\sqrt{\omega/2\alpha_2}X_2 + \sqrt{\omega/2\alpha_1}x) + \\
 & + \exp(-4\sqrt{\omega/2\alpha_1}X_1 - 2\sqrt{\omega/2\alpha_2}X_2 + \sqrt{\omega/2\alpha_1}x) \sin(\omega t - 2\sqrt{\omega/2\alpha_2}X_2 + \sqrt{\omega/2\alpha_1}x)] + \\
 & + P_2 P_4 [\exp(-2\sqrt{\omega/2\alpha_1}X_1 - 4\sqrt{\omega/2\alpha_2}X_2 + \sqrt{\omega/2\alpha_1}x) \sin(\omega t - 2\sqrt{\omega/2\alpha_1}X_1 + \sqrt{\omega/2\alpha_1}x) + \\
 & + \exp(-2\sqrt{\omega/2\alpha_1}X_1 - 4\sqrt{\omega/2\alpha_2}X_2 - \sqrt{\omega/2\alpha_1}x) \sin(\omega t + 2\sqrt{\omega/2\alpha_1}X_1 - \sqrt{\omega/2\alpha_1}x)] + \\
 & + P_3 P_4 [\exp(-2\sqrt{\omega/2\alpha_1}X_1 - 2\sqrt{\omega/2\alpha_2}X_2 + \sqrt{\omega/2\alpha_1}x) \sin(\omega t - 2\sqrt{\omega/2\alpha_1}X_1 + 2\sqrt{\omega/2\alpha_2}X_2 + \sqrt{\omega/2\alpha_1}x) + \\
 & + \exp(-2\sqrt{\omega/2\alpha_1}X_1 - 2\sqrt{\omega/2\alpha_2}X_2 - \sqrt{\omega/2\alpha_1}x) \sin(\omega t + 2\sqrt{\omega/2\alpha_1}X_1 - 2\sqrt{\omega/2\alpha_2}X_2 - \sqrt{\omega/2\alpha_1}x)] +
 \end{aligned}$$

$$\begin{aligned}
& + P_2^2 [\exp(-4\sqrt{\omega/2\alpha_1}X_1 - 4\sqrt{\omega/2\alpha_2}X_2 + \sqrt{\omega/2\alpha_1}x) \sin(\omega t + \sqrt{\omega/2\alpha_1}x)] + \\
& + P_3^2 [\exp(-4\sqrt{\omega/2\alpha_1}X_1 + \sqrt{\omega/2\alpha_1}x) \sin(\omega t + \sqrt{\omega/2\alpha_1}x)] + \\
& + P_4^2 [\exp(-4\sqrt{\omega/2\alpha_2}X_2 - \sqrt{\omega/2\alpha_1}x) \sin(\omega t - \sqrt{\omega/2\alpha_1}x)] \} \quad (10)
\end{aligned}$$

$$\begin{aligned}
T_2 = \frac{A_0}{D} (P_2 + P_4) \exp[-\sqrt{\omega/2\alpha_1}X_1 - \sqrt{\omega/2\alpha_2}(X_2 + X_3 - x)] \{ \sin[\omega t - \sqrt{\omega/2\alpha_1}X_1 - \sqrt{\omega/2\alpha_2}(X_2 + X_3 - x)] + \\
+ P_2 \exp[-2\sqrt{\omega/2\alpha_1}X_1 - 2\sqrt{\omega/2\alpha_2}X_2] \sin[\omega t + \sqrt{\omega/2\alpha_1}X_1 - \sqrt{\omega/2\alpha_2}(X_1 - x)] + \\
+ P_3 \exp[-2\sqrt{\omega/2\alpha_1}X_1] \sin[\omega t + \sqrt{\omega/2\alpha_1}X_1 - \sqrt{\omega/2\alpha_2}(X_2 + X_3 - x)] + \\
+ P_4 \exp[-2\sqrt{\omega/2\alpha_2}X_2] \sin[\omega t - \sqrt{\omega/2\alpha_1}X_1 - \sqrt{\omega/2\alpha_2}(X_1 - x)] \} + \\
+ \frac{A_0}{D} (1 + P_3) \exp[-\sqrt{\omega/2\alpha_1}X_1 - \sqrt{\omega/2\alpha_2}(X_1 - x)] \{ \sin[\omega t - \sqrt{\omega/2\alpha_1}X_1 + \sqrt{\omega/2\alpha_2}(X_1 - x)] + \\
+ P_2 \exp[-2\sqrt{\omega/2\alpha_1}X_1 - 2\sqrt{\omega/2\alpha_2}X_2] \sin(\omega t + \sqrt{\omega/2\alpha_1}X_1 + \sqrt{\omega/2\alpha_2}(X_2 + X_3 - x)] + \\
+ P_3 \exp[-2\sqrt{\omega/2\alpha_1}X_1] \sin[\omega t + \sqrt{\omega/2\alpha_1}X_1 + \sqrt{\omega/2\alpha_2}(X_1 - x)] + \\
+ P_4 \exp[-2\sqrt{\omega/2\alpha_2}X_2] \sin[\omega t - \sqrt{\omega/2\alpha_1}X_1 + \sqrt{\omega/2\alpha_2}(X_2 + X_3 - x)] \} \quad (11)
\end{aligned}$$

$$\begin{aligned}
T_3 = \frac{A_0 P_1}{D} \exp[-\sqrt{\omega/2\alpha_1}X_1 - \sqrt{\omega/2\alpha_2}X_2 + \sqrt{\omega/2\alpha_3}(X_3 - x)] \{ \sin(\omega t - \sqrt{\omega/2\alpha_1}X_1 - \sqrt{\omega/2\alpha_2}X_2 + \sqrt{\omega/2\alpha_3}(X_3 - x)) + \\
+ P_2 \exp[-2\sqrt{\omega/2\alpha_1}X_1 - 2\sqrt{\omega/2\alpha_2}X_2] \sin[\omega t + \sqrt{\omega/2\alpha_1}X_1 + \sqrt{\omega/2\alpha_2}X_2 + \sqrt{\omega/2\alpha_3}(X_3 - x)] + \\
+ P_3 \exp[-2\sqrt{\omega/2\alpha_1}X_1] \sin[\omega t + \sqrt{\omega/2\alpha_1}X_1 - \sqrt{\omega/2\alpha_2}X_2 + \sqrt{\omega/2\alpha_3}(X_3 - x)] + \\
+ P_4 \exp[-2\sqrt{\omega/2\alpha_2}X_2] \sin[\omega t - \sqrt{\omega/2\alpha_1}X_1 + \sqrt{\omega/2\alpha_2}X_2 + \sqrt{\omega/2\alpha_3}(X_3 - x)] \} \quad (12)
\end{aligned}$$

where

$$\begin{aligned}
D = 1 + 2P_2 \exp(-2\sqrt{\omega/2\alpha_1}X_1 - 2\sqrt{\omega/2\alpha_2}X_2) \cos(2\sqrt{\omega/2\alpha_1}X_1 + 2\sqrt{\omega/2\alpha_2}X_2) + \\
+ 2P_3 \exp(-2\sqrt{\omega/2\alpha_1}X_1) \cos(2\sqrt{\omega/2\alpha_1}X_1) + 2P_4 \exp(-2\sqrt{\omega/2\alpha_2}X_2) \cos(2\sqrt{\omega/2\alpha_2}X_2) \\
+ 2P_2P_3 \exp(-4\sqrt{\omega/2\alpha_1}X_1 - 2\sqrt{\omega/2\alpha_2}X_2) \cos(2\sqrt{\omega/2\alpha_2}X_2) + \\
+ 2P_2P_4 \exp(-2\sqrt{\omega/2\alpha_1}X_1 - 4\sqrt{\omega/2\alpha_2}X_2) \cos(2\sqrt{\omega/2\alpha_1}X_1) + \\
+ 2P_3P_4 \exp(-2\sqrt{\omega/2\alpha_1}X_1 - 2\sqrt{\omega/2\alpha_2}X_2) \cos(2\sqrt{\omega/2\alpha_1}X_1 - 2\sqrt{\omega/2\alpha_2}X_2) \\
+ P_2^2 \exp(-4\sqrt{\omega/2\alpha_1}X_1 - 4\sqrt{\omega/2\alpha_2}X_2) + P_3^2 \exp(-4\sqrt{\omega/2\alpha_1}X_1) + P_4^2 \exp(-4\sqrt{\omega/2\alpha_2}X_2) \quad (13)
\end{aligned}$$

and

$$\begin{aligned}
 P_1 &= \frac{4\beta_1\beta_2}{\beta_2^2\beta_3 + \beta_1\beta_2 + \beta_2^2 + \beta_1\beta_3} \\
 P_2 &= \frac{-\beta_2\beta_3 + \beta_1\beta_2 + \beta_2^2 - \beta_1\beta_3}{\beta_2\beta_3 + \beta_1\beta_2 + \beta_2^2 + \beta_1\beta_3} \\
 P_3 &= \frac{-\beta_2\beta_3 + \beta_1\beta_2 - \beta_2^2 + \beta_1\beta_3}{\beta_2\beta_3 + \beta_1\beta_2 + \beta_2^2 + \beta_1\beta_3} \\
 P_4 &= \frac{\beta_2\beta_3 + \beta_1\beta_2 - \beta_2^2 - \beta_1\beta_3}{\beta_2\beta_3 + \beta_1\beta_2 + \beta_2^2 + \beta_1\beta_3}
 \end{aligned} \tag{14}$$

The temperature is a sinusoidal function of time at all depths. It is useful to have the solutions in the form $T = A \sin(\omega t + \phi)$, i.e. in terms of the amplitude and phase of the fluctuations. We write $A = \frac{A_0}{D} \sqrt{B_1^2 + C_1^2}$ and $\phi = -\tan^{-1}(B_1/C_1)$, and find that the B_1 and C_1 are given by the following expressions.

$$\begin{aligned}
 B_1 &= \exp(-\sqrt{\omega/2\alpha_1}x) \sin(\sqrt{\omega/2\alpha_1}x) + P_2 [\exp(-2\sqrt{\omega/2\alpha_1}X_1 - 2\sqrt{\omega/2\alpha_2}X_2 + \sqrt{\omega/2\alpha_1}x) - \\
 &\quad - \exp(-2\sqrt{\omega/2\alpha_1}X_1 - 2\sqrt{\omega/2\alpha_2}X_2 - \sqrt{\omega/2\alpha_1}x)] \sin(2\sqrt{\omega/2\alpha_1}X_1 + 2\sqrt{\omega/2\alpha_2}X_2 - \sqrt{\omega/2\alpha_1}x) + \\
 &\quad + P_3 [\exp(-2\sqrt{\omega/2\alpha_1}X_1 + \sqrt{\omega/2\alpha_1}x) - \exp(-2\sqrt{\omega/2\alpha_1}X_1 - \sqrt{\omega/2\alpha_1}x)] \sin(2\sqrt{\omega/2\alpha_1}X_1 - \sqrt{\omega/2\alpha_1}x) + \\
 &\quad + 2P_4 \exp(-2\sqrt{\omega/2\alpha_2}X_2 - \sqrt{\omega/2\alpha_1}x) \cos(2\sqrt{\omega/2\alpha_2}X_2) \sin\sqrt{\omega/2\alpha_1}x \\
 &\quad - 2P_2P_3 \exp(-4\sqrt{\omega/2\alpha_1}X_1 - 2\sqrt{\omega/2\alpha_2}X_2 + \sqrt{\omega/2\alpha_1}x) \cos(2\sqrt{\omega/2\alpha_2}X_2) \sin\sqrt{\omega/2\alpha_1}x \\
 &\quad + P_2P_4 [\exp(-2\sqrt{\omega/2\alpha_1}X_1 - 4\sqrt{\omega/2\alpha_2}X_2 + \sqrt{\omega/2\alpha_1}x) - \exp(-2\sqrt{\omega/2\alpha_1}X_1 - 4\sqrt{\omega/2\alpha_2}X_2 - \sqrt{\omega/2\alpha_1}x)] x \\
 &\quad \times \sin(2\sqrt{\omega/2\alpha_1}X_1 - \sqrt{\omega/2\alpha_1}x) + P_3P_4 [\exp(-2\sqrt{\omega/2\alpha_1}X_1 - 2\sqrt{\omega/2\alpha_2}X_2 + \sqrt{\omega/2\alpha_1}x) - \\
 &\quad - \exp(-2\sqrt{\omega/2\alpha_1}X_1 - 2\sqrt{\omega/2\alpha_2}X_2 - \sqrt{\omega/2\alpha_1}x)] \sin(2\sqrt{\omega/2\alpha_1}X_1 - 2\sqrt{\omega/2\alpha_2}X_2 - \sqrt{\omega/2\alpha_1}x) \\
 &\quad - P_2^2 \exp(-4\sqrt{\omega/2\alpha_1}X_1 - 4\sqrt{\omega/2\alpha_2}X_2 + \sqrt{\omega/2\alpha_1}x) \sin\sqrt{\omega/2\alpha_1}x \\
 &\quad - P_3^2 \exp(-4\sqrt{\omega/2\alpha_1}X_1 + \sqrt{\omega/2\alpha_1}x) \sin\sqrt{\omega/2\alpha_1}x + P_4^2 \exp(-4\sqrt{\omega/2\alpha_2}X_2 - \sqrt{\omega/2\alpha_1}x) \sin\sqrt{\omega/2\alpha_1}x
 \end{aligned} \tag{15}$$

$$\begin{aligned}
C_1 = & \exp(-\sqrt{\omega/2\alpha_1}x) \cos \sqrt{\omega/2\alpha_1}x + P_2 [\exp(-2\sqrt{\omega/2\alpha_1}X_1 - 2\sqrt{\omega/2\alpha_2}X_2 + \sqrt{\omega/2\alpha_1}x) + \\
& + \exp(-2\sqrt{\omega/2\alpha_1}X_1 - 2\sqrt{\omega/2\alpha_2}X_2 - \sqrt{\omega/2\alpha_1}x)] \cos(2\sqrt{\omega/2\alpha_1}X_1 + 2\sqrt{\omega/2\alpha_2}X_2 - \sqrt{\omega/2\alpha_1}x) + \\
& + P_3 [\exp(-2\sqrt{\omega/2\alpha_1}X_1 + \sqrt{\omega/2\alpha_1}x) + \exp(-2\sqrt{\omega/2\alpha_1}X_1 - \sqrt{\omega/2\alpha_1}x)] \cos(2\sqrt{\omega/2\alpha_1}X_1 - \sqrt{\omega/2\alpha_1}x) + \\
& + 2P_4 \exp(-2\sqrt{\omega/2\alpha_2}X_2 - \sqrt{\omega/2\alpha_1}x) \cos(2\sqrt{\omega/2\alpha_2}X_2) \cos \sqrt{\omega/2\alpha_1}x \\
& + 2P_2P_3 \exp(-4\sqrt{\omega/2\alpha_1}X_1 - 2\sqrt{\omega/2\alpha_2}X_2 + \sqrt{\omega/2\alpha_1}x) \cos(2\sqrt{\omega/2\alpha_2}X_2) \cos \sqrt{\omega/2\alpha_1}x \\
& + P_2P_4 [\exp(-2\sqrt{\omega/2\alpha_1}X_1 - 4\sqrt{\omega/2\alpha_2}X_2 + \sqrt{\omega/2\alpha_1}x) + \exp(-2\sqrt{\omega/2\alpha_1}X_1 - 4\sqrt{\omega/2\alpha_2}X_2 - \sqrt{\omega/2\alpha_1}x)] \times \\
& \times \cos(2\sqrt{\omega/2\alpha_1}X_1 - \sqrt{\omega/2\alpha_1}x) + P_3P_4 [\exp(-2\sqrt{\omega/2\alpha_1}X_1 - 2\sqrt{\omega/2\alpha_2}X_2 + \sqrt{\omega/2\alpha_1}x) + \\
& + \exp(-2\sqrt{\omega/2\alpha_1}X_1 - 2\sqrt{\omega/2\alpha_2}X_2 - \sqrt{\omega/2\alpha_1}x)] \cos(2\sqrt{\omega/2\alpha_1}X_1 - 2\sqrt{\omega/2\alpha_2}X_2 - \sqrt{\omega/2\alpha_1}x) \\
& + P_2^2 \exp(-4\sqrt{\omega/2\alpha_1}X_1 - 4\sqrt{\omega/2\alpha_2}X_2 + \sqrt{\omega/2\alpha_1}x) \cos \sqrt{\omega/2\alpha_1}x \\
& + P_3^2 \exp(-4\sqrt{\omega/2\alpha_1}X_1 + \sqrt{\omega/2\alpha_1}x) \cos \sqrt{\omega/2\alpha_1}x + P_4^2 \exp(-4\sqrt{\omega/2\alpha_2}X_2 - \sqrt{\omega/2\alpha_1}x) \cos \sqrt{\omega/2\alpha_1}x
\end{aligned} \tag{16}$$

$$\begin{aligned}
B_2 = & (P_2 + P_4) \exp[-\sqrt{\omega/2\alpha_1}X_1 - \sqrt{\omega/2\alpha_2}(X_2 + X_3 - x)] \{ \sin[\sqrt{\omega/2\alpha_1}X_1 + \sqrt{\omega/2\alpha_2}(X_2 + X_3 - x)] \\
& - P_2 \exp(-2\sqrt{\omega/2\alpha_1}X_1 - 2\sqrt{\omega/2\alpha_2}X_2) \sin[\sqrt{\omega/2\alpha_1}X_1 - \sqrt{\omega/2\alpha_2}(X_1 - x)] \\
& - P_3 \exp(-2\sqrt{\omega/2\alpha_1}X_1) \sin[\sqrt{\omega/2\alpha_1}X_1 - \sqrt{\omega/2\alpha_2}(X_2 + X_3 - x)] \\
& + P_4 \exp(-2\sqrt{\omega/2\alpha_2}X_2) \sin[\sqrt{\omega/2\alpha_1}X_1 - \sqrt{\omega/2\alpha_2}(X_1 - x)] \} \\
& + (1 + P_3) \exp[-\sqrt{\omega/2\alpha_1}X_1 + \sqrt{\omega/2\alpha_2}(X_1 - x)] \{ \sin[\sqrt{\omega/2\alpha_1}X_1 - \sqrt{\omega/2\alpha_2}(X_1 - x)] - \\
& - P_2 \exp(-2\sqrt{\omega/2\alpha_1}X_1 - 2\sqrt{\omega/2\alpha_2}X_2) \sin[\sqrt{\omega/2\alpha_1}X_1 + \sqrt{\omega/2\alpha_2}(X_2 + X_3 - x)] \\
& - P_3 \exp(-2\sqrt{\omega/2\alpha_1}X_1) \sin[\sqrt{\omega/2\alpha_1}X_1 + \sqrt{\omega/2\alpha_2}(X_1 - x)] \\
& + P_4 \exp(-2\sqrt{\omega/2\alpha_2}X_2) \sin[\sqrt{\omega/2\alpha_1}X_1 - \sqrt{\omega/2\alpha_2}(X_2 + X_3 - x)] \}
\end{aligned} \tag{17}$$

$$\begin{aligned}
C_2 = & (P_2 + P_4) \exp[-\sqrt{\omega/2\alpha_1}X_1 - \sqrt{\omega/2\alpha_2}(X_2 + X_3 - x)] \{ \cos[\sqrt{\omega/2\alpha_1}X_1 + \sqrt{\omega/2\alpha_2}(X_2 + X_3 - x)] \\
& + P_2 \exp(-2\sqrt{\omega/2\alpha_1}X_1 - 2\sqrt{\omega/2\alpha_2}X_2) \cos[\sqrt{\omega/2\alpha_1}X_1 - \sqrt{\omega/2\alpha_2}(X_1 - x)] \\
& + P_3 \exp(-2\sqrt{\omega/2\alpha_1}X_1) \cos[\sqrt{\omega/2\alpha_1}X_1 - \sqrt{\omega/2\alpha_2}(X_2 + X_3 - x)] \\
& + P_4 \exp(-2\sqrt{\omega/2\alpha_2}X_2) \cos[\sqrt{\omega/2\alpha_1}X_1 + \sqrt{\omega/2\alpha_2}(X_1 - x)] \} \\
& + (1 + P_3) \exp[-\sqrt{\omega/2\alpha_1}X_1 + \sqrt{\omega/2\alpha_2}(X_1 - x)] \{ \cos[\sqrt{\omega/2\alpha_1}X_1 - \sqrt{\omega/2\alpha_2}(X_1 - x)] \\
& + P_2 \exp(-2\sqrt{\omega/2\alpha_1}X_1 - 2\sqrt{\omega/2\alpha_2}X_2) \cos[\sqrt{\omega/2\alpha_1}X_1 + \sqrt{\omega/2\alpha_2}(X_2 + X_3 - x)] \\
& + P_3 \exp(-2\sqrt{\omega/2\alpha_1}X_1) \cos[\sqrt{\omega/2\alpha_1}X_1 + \sqrt{\omega/2\alpha_2}(X_1 - x)] \\
& + P_4 \exp(-2\sqrt{\omega/2\alpha_2}X_2) \cos[\sqrt{\omega/2\alpha_1}X_1 - \sqrt{\omega/2\alpha_2}(X_2 + X_3 - x)] \}
\end{aligned} \tag{18}$$

$$\begin{aligned}
B_3 = & P_1 \exp[-\sqrt{\omega/2\alpha_1}X_1 - \sqrt{\omega/2\alpha_2}X_2 - \sqrt{\omega/2\alpha_3}(X_3 - x)] \{ \sin[\sqrt{\omega/2\alpha_1}X_1 + \sqrt{\omega/2\alpha_2}X_2 - \sqrt{\omega/2\alpha_3}(X_3 - x)] \\
& - P_2 \exp(-2\sqrt{\omega/2\alpha_1}X_1 - 2\sqrt{\omega/2\alpha_2}X_2) \sin[\sqrt{\omega/2\alpha_1}X_1 + \sqrt{\omega/2\alpha_2}X_2 + \sqrt{\omega/2\alpha_3}(X_3 - x)] \\
& - P_3 \exp(-2\sqrt{\omega/2\alpha_1}X_1) \sin[\sqrt{\omega/2\alpha_1}X_1 - \sqrt{\omega/2\alpha_2}X_2 + \sqrt{\omega/2\alpha_3}(X_3 - x)] \\
& + P_4 \exp(-2\sqrt{\omega/2\alpha_2}X_2) \sin[\sqrt{\omega/2\alpha_1}X_1 - \sqrt{\omega/2\alpha_2}X_2 - \sqrt{\omega/2\alpha_3}(X_3 - x)] \} \quad (19)
\end{aligned}$$

$$\begin{aligned}
C_3 = & P_1 \exp[-\sqrt{\omega/2\alpha_1}X_1 - \sqrt{\omega/2\alpha_2}X_2 - \sqrt{\omega/2\alpha_3}(X_3 - x)] \{ \cos[\sqrt{\omega/2\alpha_1}X_1 + \sqrt{\omega/2\alpha_2}X_2 - \sqrt{\omega/2\alpha_3}(X_3 - x)] \\
& + P_2 \exp(-2\sqrt{\omega/2\alpha_1}X_1 - 2\sqrt{\omega/2\alpha_2}X_2) \cos[\sqrt{\omega/2\alpha_1}X_1 + \sqrt{\omega/2\alpha_2}X_2 + \sqrt{\omega/2\alpha_3}(X_3 - x)] \\
& + P_3 \exp(-2\sqrt{\omega/2\alpha_1}X_1) \cos[\sqrt{\omega/2\alpha_1}X_1 - \sqrt{\omega/2\alpha_2}X_2 + \sqrt{\omega/2\alpha_3}(X_3 - x)] \\
& + P_4 \exp(-2\sqrt{\omega/2\alpha_2}X_2) \cos[\sqrt{\omega/2\alpha_1}X_1 - \sqrt{\omega/2\alpha_2}X_2 - \sqrt{\omega/2\alpha_3}(X_3 - x)] \} \quad (20)
\end{aligned}$$

An alternative way of expressing the solutions in the middle layer and in the substratum leads to results which are simpler in appearance. In the first case, one may use Lachenbruch's (1959) solution for the two-layer problem, with amplitude and phase at the surface calculated from equations (17) and (18) at $x = X_1$. In the substratum one may use the simple solution for a uniform half space (Carslaw and Jaeger, 1959, p. 65), with surface amplitude and phase calculated from (19) and (20) at $x = X_3$. The apparent simplification achieved in this way proves to be of little value for practical calculation, however. A number of terms which are independent of x , such as those on the right side of (13), must be evaluated in order to obtain numerical results in the upper layer and at the interfaces. Once this is done it seems simpler to continue to use the three-layer theory rather than evaluating new expressions which appear in the two-layer theory, and which differ from those already evaluated. The extreme simplicity of the expression for temperature in a homogeneous medium, however, makes the alternative procedure more attractive than the use of equation (12) in the substratum.

The three-layer theory leads to expressions which are far too cumbersome for hand calculation. Numerical results are easily and rapidly obtained by a digital computer, however. Use of the exact theory insures that no unwanted initial transients affect the results. If finite difference methods are used, assurance of freedom from transients is secured only by repeatedly cycling the calculation, a procedure which is far more costly in machine time than is evaluating the exact theory.

B. Applications

In order to apply the theory developed above to the lunar surface, the parameters of the problem must either be fixed, or their ranges must be restricted by estimate or by lunar observations. There are eight independent parameters (two thermal constants for each layer plus the thickness of the upper two layers), since density and heat capacity always occur in the equations as the product ρc and can be considered a single parameter. Nevertheless a very large number of permutations of values remains, and it is important to fix as many parameters as possible.

We shall take c equal to 0.2 cal/gm °C in all models; this value is appropriate to all common silicate materials under lunar surface conditions. Fixing c does not of course reduce the number of parameters unless ρ is also fixed. Perhaps the best-known lunar parameter is the thermal inertia, β , of the surface layer, which is known from infrared temperature measurements during a lunation to be about 0.0023 cal/cm² °C sec^{1/2} (see for example, Sinton, 1961, p. 411). From this result we take the product $K \rho c$ for the lunar surface to be, nearly enough, 5×10^{-6} cal²/cm⁴ °C²sec. The very low value of the thermal inertia is the principal evidence that the lunar surface is composed of granular material.

Analysis of radar echoes from the moon leads eventually to a determination of the product of density and dielectric constant. Since the latter quantity varies little among common silicates, the density may be inferred from these results. According to Evans' (1961) summary, material with the properties of loose sand would fit the radar data, i.e. a density between 1 and 2 gm/cm³ would be expected. On the other hand, the radar reflections may originate from a level beneath the optically defined surface. Lower

surface densities would then be possible and would be the automatic consequences of several postulated models of lunar surface structure (Hibbs, 1963; Warren, 1963; Hapke, 1964). We shall consider models with ρ ranging from 0.1 to 2.0 gm/cm³. Since c and β are regarded as fixed by other considerations, a choice of ρ also fixes K for the particular model of the surface layer.

We have no direct information about the properties of the subsurface layers. We shall assume that the substratum consists of unfractured basic rock; appropriate properties are shown in table 2. The intermediate layer is presumably made up of rubble, with properties between those of the surface layer and the substratum. Three possibilities have been considered in order to indicate the effects to be expected from such a layer. They do not exhaust the possible range of properties; models with the surface layer resting directly on a solid substratum or with an infinite thickness of surface material may be considered limiting cases. The thermal properties that have been considered in the following numerical calculations are collected in table 2.

It is useful at the outset to recognize two limiting types of amplitude - depth relations. In a homogeneous medium the amplitude of the temperature oscillation decreases with depth according to the relation $A = A_0 \exp(-\sqrt{\omega/2\alpha} x)$. The exponential damping law is obeyed far from the lower contact of a thick surface layer of low thermal diffusivity. A different extreme is encountered if the density of the material becomes very small. The term in the equation of heat conduction containing the time derivative then becomes negligible, and the amplitude is found to decrease linearly with depth. The numerical results which follow contain examples of both types of behavior.

Table 2. Properties of layers.

K cal/cm sec°C	ρ gm/cm ³	c cal/gm°C	α cm ² /sec	β cal/cm ² °C sec ^{1/2}
I. Surface layer.				
1. 2.5×10^{-4}	0.1	0.2	1.25×10^{-2}	2.24×10^{-3}
2. 5×10^{-5}	0.5	0.2	5.0×10^{-4}	2.24×10^{-3}
3. 2.5×10^{-5}	1.0	0.2	1.25×10^{-4}	2.24×10^{-3}
4. 1.25×10^{-5}	2.0	0.2	3.12×10^{-5}	2.24×10^{-3}
II. Intermediate layer.				
A 1×10^{-3}	1.0	0.2	5.0×10^{-3}	1.41×10^{-2}
B 1×10^{-3}	2.0	0.2	2.5×10^{-3}	2.00×10^{-2}
C 2×10^{-3}	2.5	0.2	4.0×10^{-3}	3.16×10^{-2}
III. Substratum.				
5×10^{-3}	3.0	0.2	8.33×10^{-3}	5.48×10^{-2}
IV. Blanket materials.				
SI-10 2.69×10^{-7}	0.032	0.2	4.20×10^{-5}	4.15×10^{-5}
SI-91 4.14×10^{-8}	0.120	0.2	1.72×10^{-6}	3.15×10^{-5}
Plastic 1.0×10^{-4}	1.3	0.2	3.85×10^{-4}	5.10×10^{-3}

In the calculations A_0 was given the value 314°C . This is not the amplitude of the temperature fluctuation at the lunar surface, but rather is twice the amplitude of the fundamental mode in the Fourier analysis of lunar surface temperature given by Sinton (1961). This term is more interesting than the higher harmonics because it is about 5 times as large and because it penetrates the most deeply. Doubling the amplitude gives the total range of temperature directly.

Some typical results are shown in figs. 1 through 6. The curves of amplitude and phase vs. depth have characteristic shapes; the sharp drops in the curves as interfaces are approached are particularly noteworthy. Study of both amplitude and phase seems to give little more information than study of amplitude alone, although any program of temperature measurement would automatically yield both quantities.

The amplitudes decrease exponentially near the tops of layers about a meter or more in thickness. The law of decrease is the same as in a semi-infinite region, and the thermal diffusivity of the layer can be obtained from the damping observed. Where the exponential law is not obeyed, the properties of more than one layer are involved and it is doubtful whether they can ever be uniquely untangled. In the situations where a linear law applies (cf. figs. 1 and 2), the properties of the lower layers assume special importance relative to the upper layer in which the linear damping occurs.

In a case in which measurements of temperature cannot be made throughout the thickness of a layer, the proximity of an interface could be detected, if indeed one were near. No more than this qualitative result can be obtained unless the depth of the interface is also known (c.f. figs. 4, 5,

and 6). Temperatures must be measured at the interface in order to determine the properties of the underlying layer reliably, and little more than its thermal inertia can be deduced unless some penetration of the underlying layer is possible.

It is worthwhile remarking again that the above conclusions are correct only if linearization of the conduction equation is valid. This will certainly not be true close to the surface, and will only become valid at depths where the oscillations in temperature are severely damped. This depth is critically dependent on the surface material. In a homogeneous region of material 4 of table 2(I), the amplitude reaches 1 degree at a depth of 30 cm. In a homogeneous region of solid rock (substratum of Table 2) an amplitude of 1 degree occurs at a depth of 450 cm. In both cases the surface amplitude was taken to be 314 degrees, as before. The presence of layering would reduce those depths. In practice, the linear theory will probably be valid if the amplitudes are less than 10 degrees, but should be regarded with suspicion in cases of higher amplitudes.

3. STEADY PERIODIC TEMPERATURES NEAR A HOLE IN THE SURFACE LAYER

The poorly conducting lunar surface layer may locally be absent, and the substratum of higher conductivity may be exposed to high-amplitude fluctuations in temperature at the surface. Damping near such outcrops will be comparatively inefficient, and large amplitudes of the thermal wave may penetrate the substratum both laterally and vertically. We require an estimate of the extent of serious disturbance.

A simple geometrical model of an outcrop is obtained as follows. Imagine first a two-layer structure of the sort described in the last section, i.e. a uniform layer with one set of properties separated by a plane boundary from a substratum of different properties. We then remove a piece of the upper layer having the shape of a right circular cylinder, and fill the resulting hole with material of the substratum. The result is a cylindrical protuberance on the substratum extending to the original plane surface.

Analytical solutions to heat flow problems in heterogeneous regions of this degree of complexity are unknown, and recourse to numerical methods must be had. The following calculations were made from the simplest form of finite-difference approximation to the equation of heat conduction in cylindrical coordinates (see for example Carslaw and Jaeger, 1957, p. 468,470). The program written for the computer took account of different conductivities in the two layers, but did not allow for different densities and heat capacities. This simplification does not affect the qualitative conclusions drawn from the calculations. A second simplification was to assume that the surface temperature was

independent of position and varied with time in the manner shown by Sinton (1961, fig. 3). Actually the amplitude of the variation would be smaller in the hole, because of the better connection between the surface and the lunar interior there, and the extent of the perturbation of amplitudes is therefore slightly overestimated because of neglect of this effect.

Results of the calculations are shown in fig. 7 as contours of equal amplitudes. The conductivity of the surface layer is taken to be 1/10th that of the substratum. It is evident from the figure that the effect of the hole is negligible at a distance from the edge equal to its diameter, and that serious perturbations do not extend further than about half this distance. The amplitudes decrease monotonically with depth everywhere, as is shown by the fact that no contour can be intersected more than once by any vertical line. Thus there is no tendency for high-amplitude fluctuations originating in the hole to "run under" the surface layer. It may be concluded from these results that the influence of an outcrop on amplitudes does not persist for a distance greater than its diameter.

4. STEADY-STATE PERTURBATIONS OF FLUX DUE TO IRREGULARITIES IN THE THICKNESS OF THE SURFACE LAYER

If the thickness of the poorly conducting surface layer is variable, heat tends to be funneled towards thin spots in the layer and away from thick spots, a phenomenon sometimes termed thermal refraction. Refraction causes the flux observed at the surface to be high where the insulating layer is thin and low where it is thick. Some studies of terrestrial heat flow have revealed irregularities which may be attributable to thermal refraction. Errors arising from this effect may be large in cases where the conductivity contrasts are large; a good terrestrial example would be near a salt dome in poorly consolidated, fine-grained sediments.

The contrast in conductivity near the lunar surface may exceed a factor of 10 (table 2), a contrast that is considerably larger than one would expect to encounter on earth. The proportional change in flux scales according to the ratio of the conductivity of the substratum to the conductivity of the surface layer, and hence large perturbations may be expected near the lunar surface. The question was investigated quantitatively by studying the steady-state temperature distribution around cylindrical protuberances on the interface between an upper poorly conducting layer and a better conducting substratum. The problem is analogous to the investigation of amplitudes near an outcrop discussed in the last section, but with constant surface temperature. The same machine program was used, steady-state conditions being achieved by allowing the calculation to iterate until the temperatures stopped changing.

In the application of a steady-state theory to the lunar surface, it must be assumed that the periodic transients either have been avoided

by measuring heat flow in a sufficiently deep hole or have been removed by observing temperatures over at least one cycle and calculating undisturbed steady-state means. The results of this section show that even if one of these ways of removing transient effects can be followed (neither will necessarily be easy to carry out), perturbations leading to erroneous measurements of lunar heat flow may still remain.

A number of typical results are shown in fig. 8. Cases (d) and (e), in which the substratum crops out at the surface, lead to the largest perturbations, but such localities are obviously atypical and could easily be avoided. The perturbations are greatly reduced if the irregularities in the interface are completely buried as in the other cases shown, but nevertheless they are appreciable. Local variations up to about 50% may be found in all of the cases examined. The results shown in fig. 8 were calculated for a ratio of conductivities of 10; reference to table 2 shows that this value is, if anything, too low. A conductivity ratio of 20 would lead to perturbations of a factor of 2 or more, depending on whether one considers enhancement or reduction of the undisturbed flux.

In order to be useful, a measurement of lunar heat flow must lead to an estimate of mean flux in a region with dimensions measured in kilometers which is accurate to better than 20%. If the error is much greater than this the numbers will have little significance for geophysical or cosmological theory. The mean value of 10 fairly closely spaced measurements would have the required accuracy, assuming that the individual values are disturbed by no more than 50% and that the disturbances are normally distributed with zero mean value. This latter requirement implies that the probability of finding a given positive disturbance must be the same as finding a

negative disturbance of the same amount. It is not at all clear that a system of randomly distributed, small, buried craters would have this property. Furthermore systematic error would invalidate this statistical method of achieving accuracy if, for example, all of the measurements were made within a large buried crater so that all were affected by a negative disturbance.

An alternative approach is to escape the near-surface perturbations by drilling deeply enough to make the measurement beneath them. It should be possible to do this, because porosity will be eliminated or greatly reduced by the weight of overburden, and very large contrasts in conductivity will no longer be possible. Considerable depths of penetration may be required, however, since disturbed temperatures extend to a distance beneath the bottom of the anomalous region roughly equal to its diameter.

5. THE BLANKET METHOD OF MEASURING LUNAR HEAT FLOW

A. Introduction.

If a sheet of material of known thermal conductivity is placed on the lunar surface and allowed to come into thermal equilibrium, the heat flow through the surface can be determined from measurements of the thermal gradient in the sheet. A device consisting of a suitable insulating material and temperature sensors for the determination of the gradient is known as a fluxmeter, or blanket. Such devices have found meteorological application in the study of heat exchange between the ground and the atmosphere, but they have never been successfully used in the measurement of terrestrial heat flow except in thermal regions where the heat flow is orders of magnitude higher than normal.

The extreme simplicity of the blanket method makes it appear attractive as a tool for determination of lunar heat flow. Associated difficulties seem to outweigh this advantage, however, as is discussed below.

B. Simple steady-state blanket theory.

Since one has complete control over the geometry of the blanket, it is possible to select a shape that is amenable to simple theoretical treatment. A circular disc with diameter greatly exceeding thickness proves to be a convenient choice. An approximate method of treating this problem has been suggested privately by A. H. Lachenbruch, and much of the following discussion is due to him.

Consider a half space with zero initial temperature. If, starting at $t=0$, the temperature of the surface is maintained at a constant value ΔT within a circle of radius R and zero outside the circle, then beneath

the center of the circle (Lachenbruch, 1957)

$$T = \Delta T [\operatorname{erfc} x/\sqrt{4\alpha t} - \{x/\sqrt{x^2+R^2}\} \operatorname{erfc}\sqrt{x^2+R^2}/\sqrt{4\alpha t}] \quad (21)$$

where x is depth. Beneath the center, as the depth approaches zero, the vertical gradient approaches

$$\nabla T = -\Delta T [1/R \operatorname{erfc} R/\sqrt{4\alpha t} + 1/\sqrt{\pi\alpha t}] \quad (22)$$

and the heat flow approaches

$$\Delta Q = \Delta T [K/R \operatorname{erfc} R/\sqrt{4\alpha t} + \rho/\sqrt{\pi t}] \quad (23)$$

(See table 1 for definitions of symbols.) In the steady state (23) reduces to

$$\Delta Q = K \Delta T/R \quad (24)$$

As an illustration of the application of these results, consider the case of a blanket placed on the plane lunar surface. The upper surface of the blanket is supposed to be at zero, as is the lunar surface outside the blanketed area. The assumption that the steady periodic transient has somehow been removed is implicit. If the lunar flux is everywhere Q , then ΔT in (24) becomes equal to $\bar{Q}\bar{X}_b/K_b$, where \bar{X}_b is the thickness of the blanket and the subscript b denotes blanket properties. From (24) we find a perturbation of flux

$$\Delta Q/Q = 1 - Q_b/Q = \frac{\bar{X}_b K}{R K_b} \quad (25)$$

due to the blanket. This result is approximate first because the undisturbed flux Q was used to calculate ΔT , and secondly because ΔT is assumed constant when in fact it varies with radius in an unknown way. The first objection can be overcome by substituting Q_b for Q in the expression for ΔT , calculating the new disturbance, and iterating the process until it converges. For example, if $K/K_b = 10$ and $R/\bar{X}_b = 50$, we find $\Delta Q/Q = 0.2$ and $Q_b/Q = 0.8$. Substituting $\Delta T_b = 0.8 \Delta T$ for ΔT leads to $Q_b/Q = 0.84$, and a second iteration gives $Q_b/Q = 0.842$. The process evidently converges rapidly. The second objection mentioned above is inherent in the method, since edge effects are neglected. The error is small if

R/\bar{X}_b is large enough.

In order to get a quantitative idea of the meaning of "large enough" consider a second illustration of the method. A blanket is now supposed to be buried so that its upper surface coincides with the initial plane surface. The geometry is identical to that shown in figure 8(e). Again we assume uniform flux as a first approximation. The thermal gradient in the blanket is then Q/K_b , and elsewhere it is Q/K ; the corresponding temperatures at the level of the base of the blanket are $Q\bar{X}_b/K_b$ and $Q\bar{X}_b/K$ respectively. Equation (24) then gives

$$\Delta Q/Q = 1 - Q_b/Q = \frac{\bar{X}_b}{R} [K/K_b - 1] \quad (26)$$

in this case. Iteration again may be used to improve the result. This problem can also be solved by the finite-difference method used above in section 3, and a comparison of the results gives some idea of the range of applicability of the approximate method (figure 9). The finite-difference calculations agree well with equation (26) for R/\bar{X}_b greater than about 20, but iteration does not improve the agreement. The iteration process becomes unstable for R/\bar{X}_b equal to 10 or less. It appears that some compensation between the errors arising from neglected edge effects and those due to other approximations in the derivation of (26) takes place, and the use of (26) without iteration appears to give the more reliable results. Since the finite-difference calculations are probably not accurate to better than 5 per cent, the results given by the simple approach outlined here are satisfactory.

There is a second type of disturbance arising from the presence of a blanket on the lunar surface which may be treated exactly by the present method. If the albedo of the blanket does not match that of the lunar surface, the mean temperature of the top of the blanket will differ from the mean surface temperature. The disturbance of flux can be estimated directly from (23) and (24). For example, if a blanket 100 cm in radius

rests on material of conductivity 5×10^{-5} (material I(2) of table 2), then a difference in temperature of only 0.2°C produces a steady-state disturbance in flux of $0.1 \times 10^{-6} \text{ cal/cm}^2 \text{ sec}$. Such a disturbance may already be intolerably large; it becomes worse if the surface material is a better conductor or if the radius of the blanket is reduced to a more manageable figure. It will be difficult to measure the mean temperature of the lunar surface to better than 1°C , so that a serious disturbance due to mismatching albedo may go completely undetected.

C. Time-dependent problems associated with the blanket method.

It is convenient to consider separately two causes of time-dependent temperatures. One is the steady periodic regime prevailing near the lunar surface, and the other is the transient disturbance arising from the emplacement of the blanket. The latter has two sources. The blanket may not be at the same initial temperature as the lunar surface, and after emplacement the establishment of the lunar thermal gradient within the blanket changes both its temperature and that of the lunar material. The first source of disturbance can be avoided by careful planning, but the second cannot.

Steady periodic temperatures in the blanket were investigated by the methods of section 2. The blanket, taken to be 5 cm thick, was assumed to rest on a thick layer having the properties of layer 2 of table 2(I), on 50 cm of such material which rested in turn on the substratum of table 2(III), or directly on the substratum. Three kinds of blanket materials were considered (table 2(IV)). Two of them, SI-10 and SI-91, are "superinsulators" developed by Linde for the storage of cryogenic fluids. The thermal conductivity of these materials is extraordinarily low, as is shown in the table. A third blanket material was assumed to have properties corresponding roughly to those of ordinary plastics (e.g. bakelite or plexiglass).

Amplitudes and phases of the temperature variations at the bottom of the blanket are shown in table 3 for the various combinations of blanket materials and assumed lunar configurations. The amplitude-depth curve in the blanket has the same shape as the curves for the upper layer shown in figure 1a; that is, the amplitude at the center of the blanket exceeds the geometric mean of the surface amplitude (314°C) and the amplitude shown in the table. Clearly only the superinsulators are capable of reducing the fluctuation to manageable proportions (order of tens of degrees or less) in the lower half of the blanket. It is doubtful whether the mean temperature can be determined in the "plastic" blanket to sufficient accuracy. The situation is made worse by the fact that the expected gradient is inversely proportional to the conductivity of the blanket. In the superinsulators the expected gradient is on the order of $1\text{-}10^{\circ}\text{C}/\text{cm}$, whereas in the "plastic" a gradient of $10^{-2}\text{-}10^{-3}^{\circ}\text{C}/\text{cm}$ seems likely.

Hence we find that the use of superinsulators is indicated in order to eliminate the steady periodic fluctuations most effectively and to raise the mean thermal gradient to an easily measured value. But now we must consider the transient associated with blanket emplacement. We assume that the lateral dimensions of the blanket are great compared with its thickness, so that the problem can be treated as one of 1-dimensional heat flow. The blanket, occupying the region $-\underline{L} \leq \underline{x} \leq 0$, is assumed to have initial temperature \underline{T}_0 , and thermal properties indicated by the subscript \underline{b} . The lunar material (assumed uniform) has initial temperature $\underline{m}\underline{x}$, where $\underline{x} \geq 0$ equals depth, and unsubscripted properties.

Writing \bar{T} for the Laplace transform of T , as before, we find

$$\bar{T}_{\underline{b}} = \underline{T}_0/p + A \sinh q_{\underline{b}} \underline{x} + B \cosh q_{\underline{b}} \underline{x} \quad (27)$$

and

$$\bar{T} = \underline{m}\underline{x}/p + C \exp(-q\underline{x}) \quad (28)$$

Table 3. Amplitude and phases at
base of blanket 5 cm thick.

Blanket material	Substratum (table 2)	Amplitude °C	Phase
SI-10	I-2, III	4.5	-60
SI-10	I-2	4.5	-60
SI-10	III	0.2	-60
SI-91	I-2, III	0.1	-253
SI-91	I-2	0.1	-252
SI-91	III	0.004	-252
Plastic	I-2, III	274	-11
Plastic	I-2	274	-11
Plastic	III	60	-39

where A, B, C are constants independent of x . Application of initial conditions $\bar{T}_b = \bar{T}_0$ and $\bar{T} = mx$, and the conditions of continuity of temperature and flux at $x = 0$ lead to

$$A = [KqT_0(\cosh q_b L - 1) - K_m \cosh q_b L]/pD \quad (29)$$

$$B = [KqT_0 \sinh q_b L + K_b q_b T_0 - K_m \sinh q_b L]/pD \quad (30)$$

$$C = [-K_b q_b T_0(\cosh q_b L - 1) - K_m \sinh q_b L]/pD \quad (31)$$

where

$$D = -Kq \sinh q_b L - K_b q_b \cosh q_b L \quad (32)$$

Conversion of the hyperbolic functions in (29) through (32) to exponentials, and expansion of D by the binomial theorem then leads to the following expressions for the temperatures

$$\begin{aligned} T_b = T_0 & \left\{ 1 - \frac{\beta}{\beta + \beta_b} \left[\sum_{n=0}^{\infty} (M)^n \left(\operatorname{erfc} \frac{2nL-x}{\sqrt{4\alpha_b t}} - \operatorname{erfc} \frac{(2n+2)L+x}{\sqrt{4\alpha_b t}} \right) \right. \right. \\ & + M \sum_{n=0}^{\infty} (M)^n \operatorname{erfc} \frac{(2n+1)L-x}{\sqrt{4\alpha_b t}} - \sum_{n=0}^{\infty} (M)^n \operatorname{erfc} \frac{(2n+1)L+x}{\sqrt{4\alpha_b t}} \} \\ & + \frac{2K_m \sqrt{t}}{\beta + \beta_b} \left[\sum_{n=0}^{\infty} (M)^n \left(\operatorname{ierfc} \frac{2nL-x}{\sqrt{4\alpha_b t}} - \operatorname{ierfc} \frac{(2n+2)L+x}{\sqrt{4\alpha_b t}} \right) \right] \end{aligned} \quad (33)$$

$$\begin{aligned} T = T_0 & \frac{\beta_b}{\beta + \beta_b} \sum_{n=0}^{\infty} (M)^n \left[2 \operatorname{erfc} \left(\frac{(2n+1)L}{\sqrt{4\alpha_b t}} + \frac{x}{\sqrt{4\alpha t}} \right) \right. \\ & - \operatorname{erfc} \left(\frac{2nL}{\sqrt{4\alpha_b t}} + \frac{x}{\sqrt{4\alpha t}} \right) - \operatorname{erfc} \left(\frac{(2n+2)L}{\sqrt{4\alpha_b t}} + \frac{x}{\sqrt{4\alpha t}} \right) \} \\ & + \frac{2K_m \sqrt{t}}{\beta + \beta_b} \sum_{n=0}^{\infty} (M)^n \left[\operatorname{ierfc} \left(\frac{2nL}{\sqrt{4\alpha_b t}} + \frac{x}{\sqrt{4\alpha t}} \right) \right. \\ & - \operatorname{ierfc} \left(\frac{(2n+2)L}{\sqrt{4\alpha_b t}} + \frac{x}{\sqrt{4\alpha t}} \right) \left. \right] + mx \end{aligned} \quad (34)$$

Here $M = (\beta - \beta_b)/(\beta + \beta_b)$ and the other symbols are defined in table 1.

Equations (33) and (34) are most convenient to use for small values of time, but they converge for all times. Numerical values of the flux in the blanket divided by the undisturbed lunar flux are shown in figure 10 for

blankets of material SI-10 and SI-91 on dust (table 2(I)2) and substratum (table 2 (III)). In the most favorable case the flux in the blanket is less than 15% of the equilibrium flux after 1 year. This result is virtually independent of the T_o term; it arises mainly from the m term. Hence no matter how carefully the initial temperature of the blanket is matched to the mean temperature of the lunar surface, a major disturbance is caused by emplacement of the blanket, and it persists for years if the blanket is made of superinsulating material. The higher the conductivity of the substratum, the longer is the time required to reach equilibrium. The "plastic" blanket, on the other hand, achieves equilibrium within a year.

Thus we see that the two classes of time-dependent temperatures pose difficulties that appear to require mutually incompatible sets of blanket properties for their solution. In the examples given one must face either a large periodic fluctuation throughout the blanket, or a prohibitively long time for equilibrium to be established. It does not appear that the use of a blanket material with intermediate properties would solve the problem. One would then be confronted with both a large periodic fluctuation and a long time constant. The thickness of the blanket affects its thermal behavior in much the same way as its thermal diffusivity, so that no escape can be found by changing this parameter.

A final consideration about the blanket type of flux meter concerns its contact with the lunar surface. In all of the foregoing calculations it has been assumed that there is no contact resistance between the blanket and the lunar surface, a situation that is difficult to achieve in practice. The effect of uniform contact resistance is to reduce the effectiveness with which the periodic fluctuation is damped out in the blanket and to increase the time required to equilibrate with the lunar surface. Nonuniform contact resistance, which is likely to be encountered due to irregularities on the lunar surface, will in addition

cause thermal refraction within the dimensions of the blanket. This will cause the flux in the blanket to differ from point to point, necessitating a large number of temperature sensors to give a proper mean gradient. Readout is not necessarily complicated by such a requirement, since a single readout of many resistance elements in series and/or parallel to give an appropriate mean value would in all probability be feasible.

5. CONCLUSIONS

A. One-dimensional steady periodic temperatures.

A limited amount of information about the thermal properties of a layer can be obtained from a study of amplitude or phase of the thermal wave as a function of depth, if the effect of other layers is small. The latter condition can be recognized by the exponential decrease in amplitude with depth. Study of both amplitude and phase gives little or no information in addition to that provided by study of amplitude alone. When the properties of more than one layer influence the temperatures to an important degree, it may be possible to determine the properties of those layers penetrated completely by a hole. Extrapolation beyond the deepest observation of temperature is not reliable unless the depth to the next interface is accurately known independently.

B. Propagation of the thermal wave near a hole in the surface layer.

A hole or thin spot in the surface layer will let high-amplitude fluctuations leak into the substratum, where they may propagate laterally to some distance. This effect does not appear to be serious, however. The amplitudes are essentially unaffected by the presence of the hole a few meters away.

C. Thermal refraction due to irregular thickness of the surface layer.

This steady-state phenomenon is far more serious than the periodic disturbance discussed under B. Conditions very probably exist near the lunar surface which cause differences in flux of 50% or more because of thermal refraction. Such anomalies can be avoided by measuring heat flow at depths below regions causing refraction. Errors due to this effect can

largely be removed by taking the means of several closely spaced observations. It seems best to try to take advantage of both techniques, and to measure temperatures in the deepest holes practicable at several points at a given lunar site.

D. The blanket method of measuring lunar heat flow.

The following difficulties are recognized as standing in the way of a measurement of lunar heat flow by a blanket-type fluxmeter.

1. The flux is disturbed by thermal refraction due to the presence of the blanket. This effect can be kept small by choice of proper geometry for the blanket, and the correction is calculable.
2. The flux is disturbed if the albedo of the blanket does not match that of the lunar surface and a difference in mean temperature between the blanket and the surface is thereby created. This disturbance is serious if the mismatch in temperature exceeds a few tenths of degrees.
3. The blanket must be made of poorly conducting material in order to damp out the steady periodic temperature fluctuation in a reasonable thickness, and also to have a readily measurable thermal gradient set up by the lunar flux. But a blanket satisfying these requirements takes years to come into equilibrium with the lunar flux. A blanket having a manageable time constant associated with its emplacement does not satisfy the requirements imposed by the steady periodic fluctuations and the small value of flux to be measured.
4. The flux through the blanket may vary from point to point because of variable contact resistance with the lunar surface. A large number of temperature sensors would be necessary to measure a meaningful average flux.

Difficulties (2) and (3) in particular seem insuperable and make the blanket method unattractive for the measurement of lunar heat flow.

8. REFERENCES CITED

- Carslaw, H. S. and J. C. Jaeger, 1959, Conduction of heat in solids, London, Oxford Univ. Press, 510 pp.
- Hapke, B., 1964, Photometric and other laboratory studies relating to the lunar surface, in The lunar surface layer, J. W. Salisbury and P. E. Glaser eds., New York Academic Press, 532 pp.
- Hibbs, A. R., 1963, A hypothesis that the surface of the moon is covered with needle crystals, Icarus, 2, 181-186.
- Lachenbruch, A. H., 1957, Three-dimensional heat conduction in permafrost beneath heated buildings, U. S. Geol. Survey Bull. 1052-B, p. 51-69.
- _____, 1959, Periodic heat flow in a stratified medium with application to permafrost problems, U. S. Geol. Survey Bull. 1083-A, p. 1-36.
- Sinton, W. M., 1961, Temperatures on the lunar surface, in Physics and astronomy of the moon, Z. Kopal ed., New York, Academic Press, 538 pp.
- Warren, C. R., 1963, Surface material of the moon, Science, 140, 188-190.

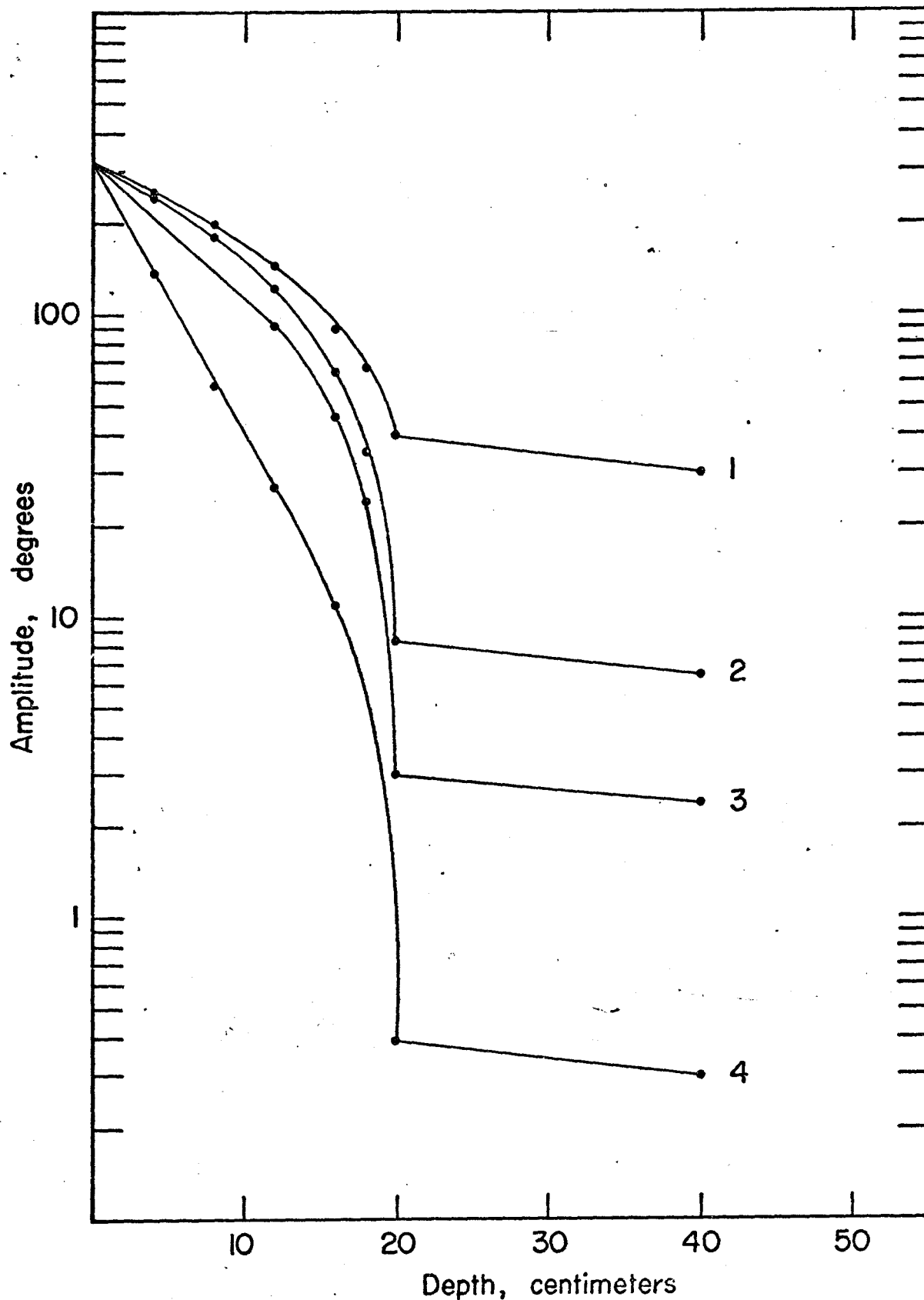


Figure 1a. Effect of properties of the surface material on amplitudes in a layer 20 cm. thick. Numbers beside the curves identify the rows in table 2 (I). Lower layer is substratum of table 2 (III).

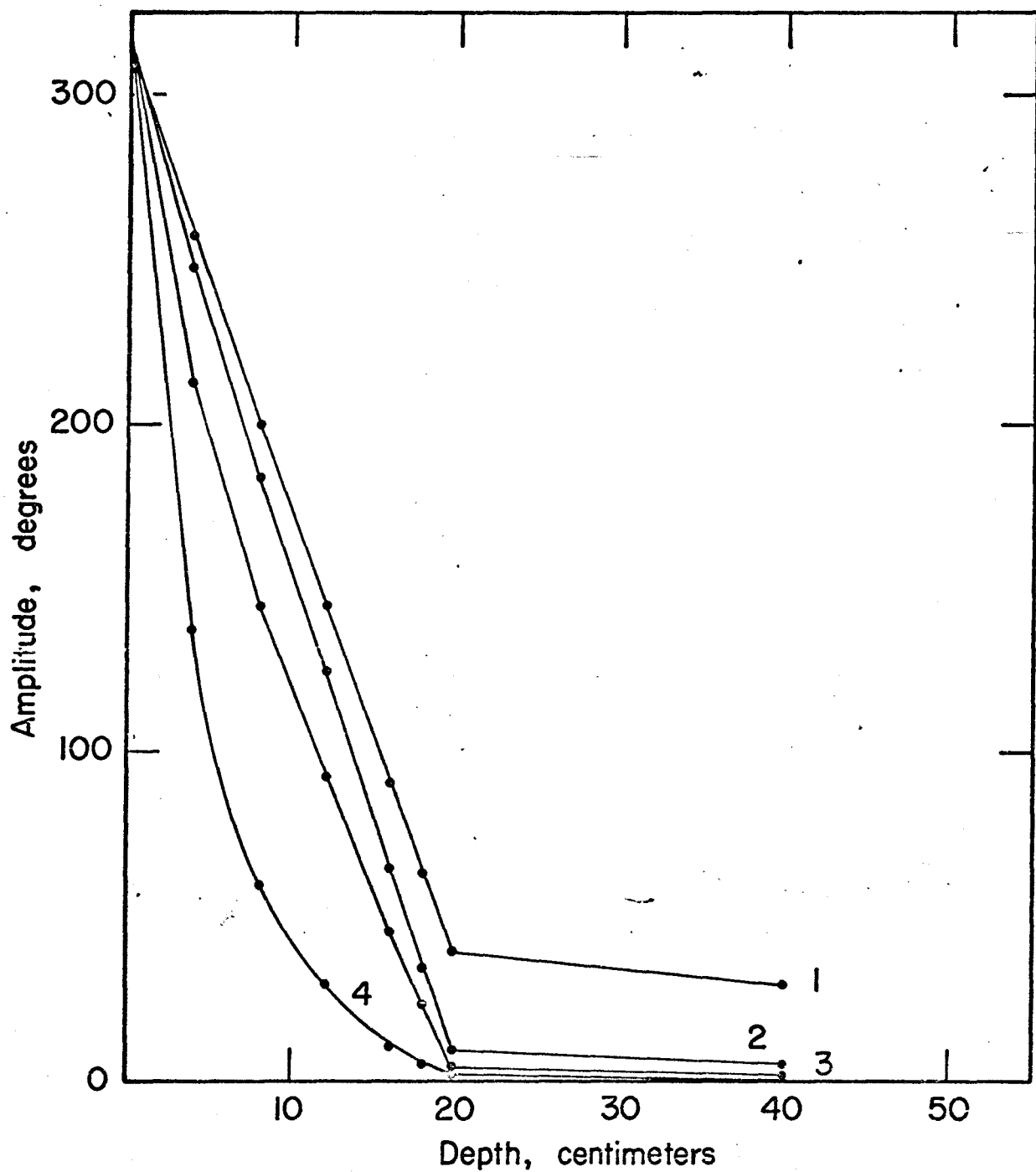


Figure 1b. Effect of properties of the surface material on amplitudes. Same as figure 1a except amplitude scale is linear.

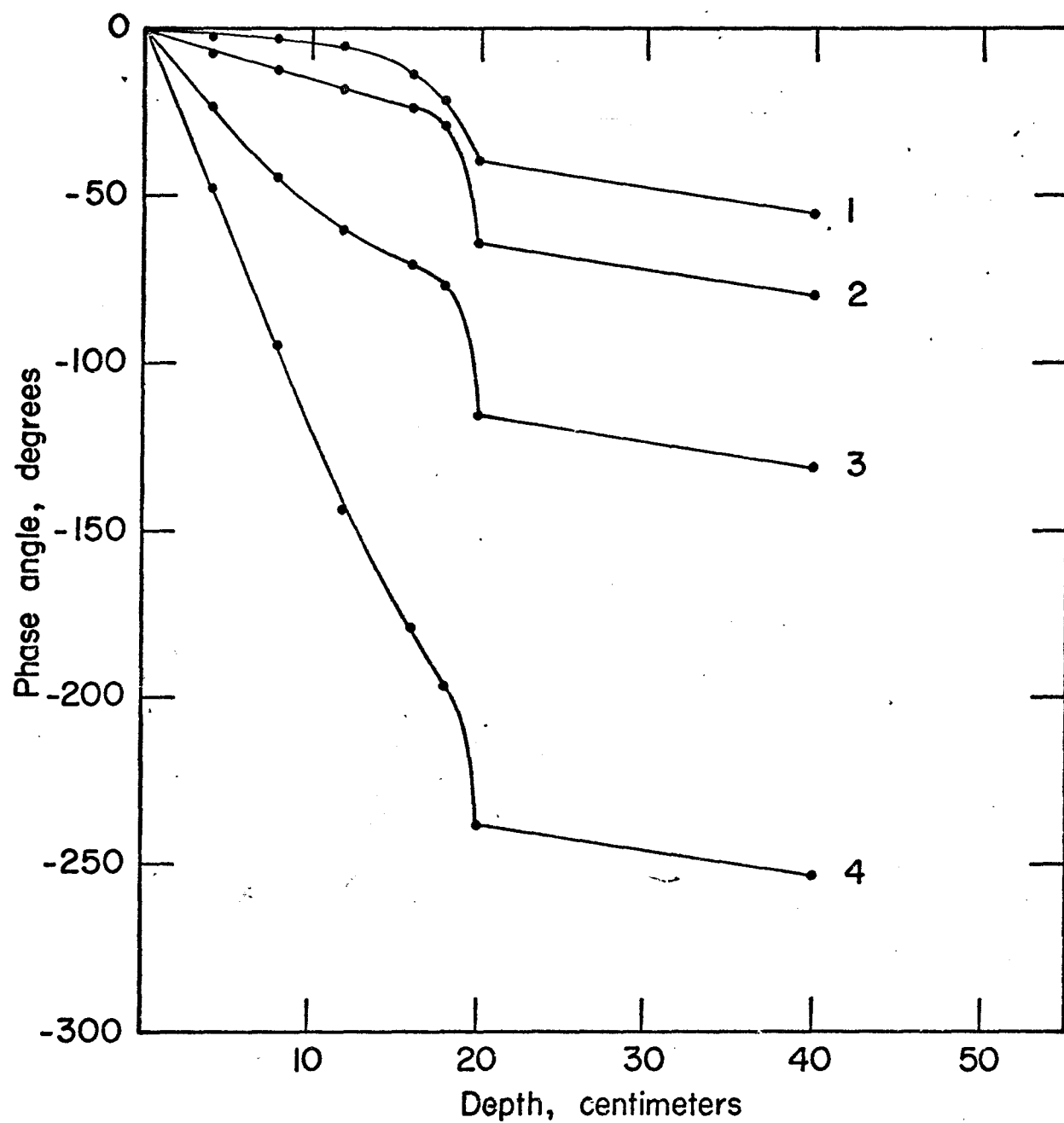


Figure 1c. Phase lags in surface layers of figure 1a.

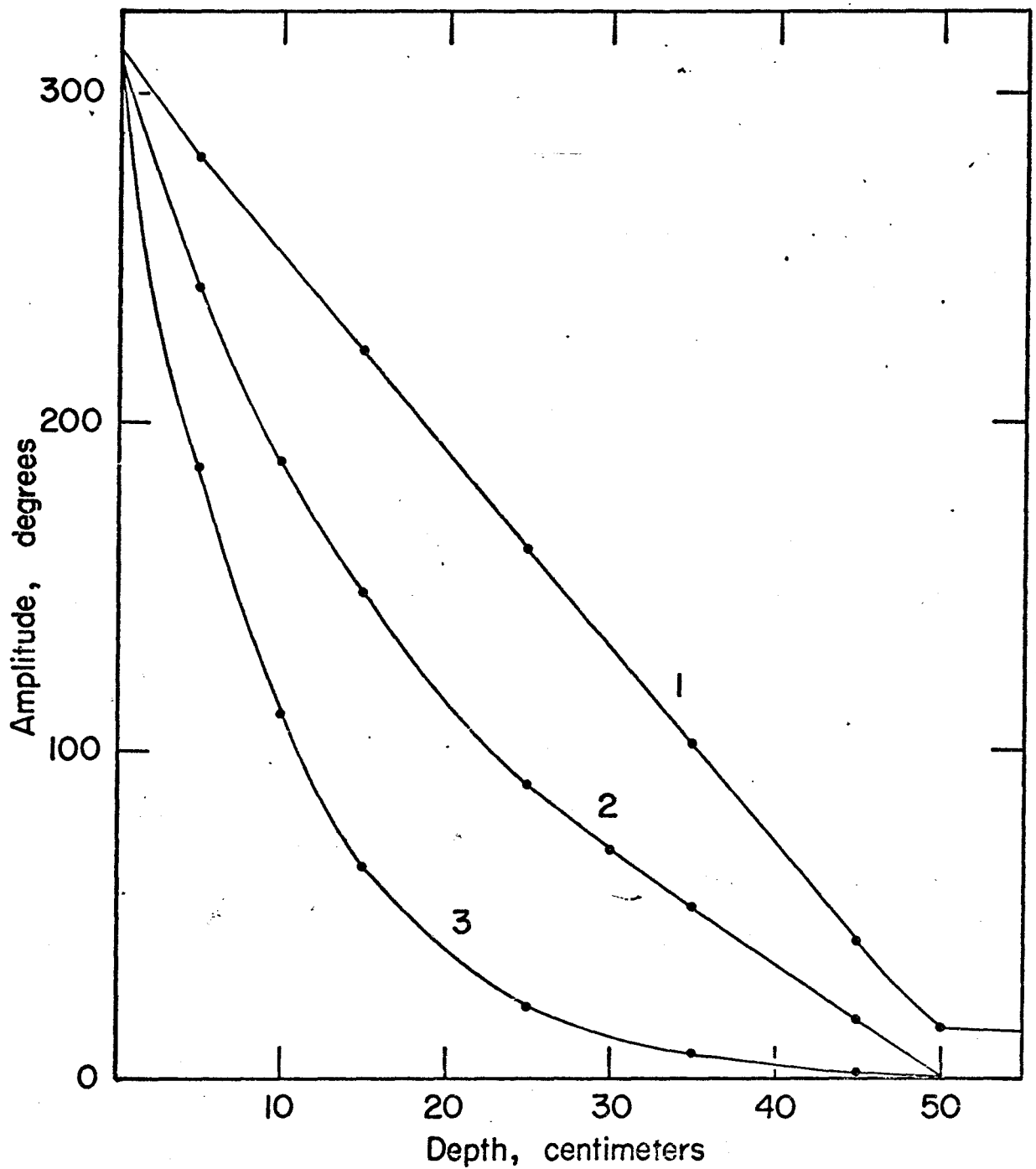


Figure 2. Amplitudes in a surface layer 50 cm. thick. Numbers beside the curves identify the rows in table 2 (I).

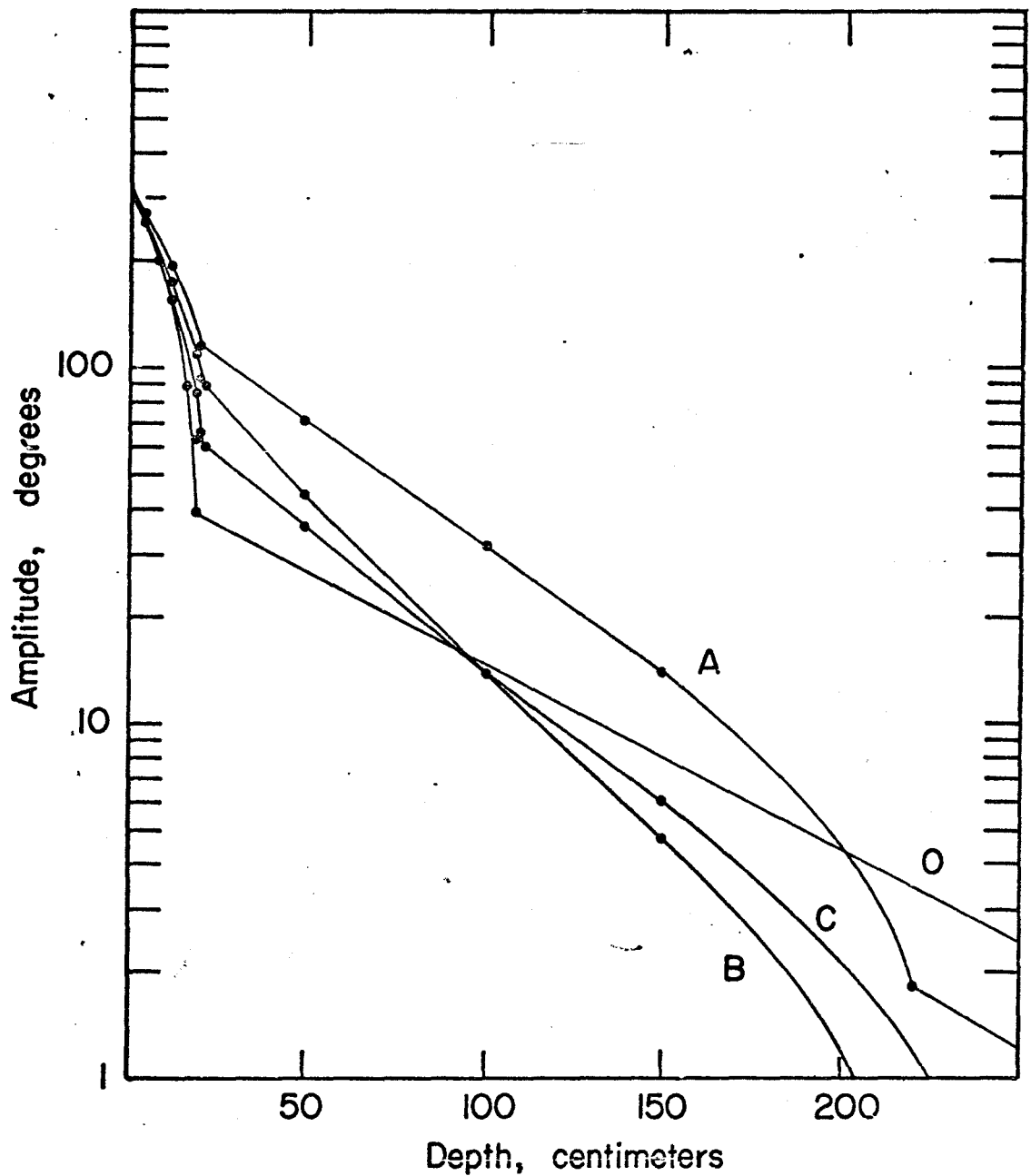


Figure 3a. Effect of properties of the intermediate layer on amplitudes. Upper layer 20 cm. thick of material I of table 2 (I). Curves A, B, C for 200 cm. thickness of materials A, B, C of table 2 (II). Curve O, no intermediate layer, surface material rests directly on substratum.

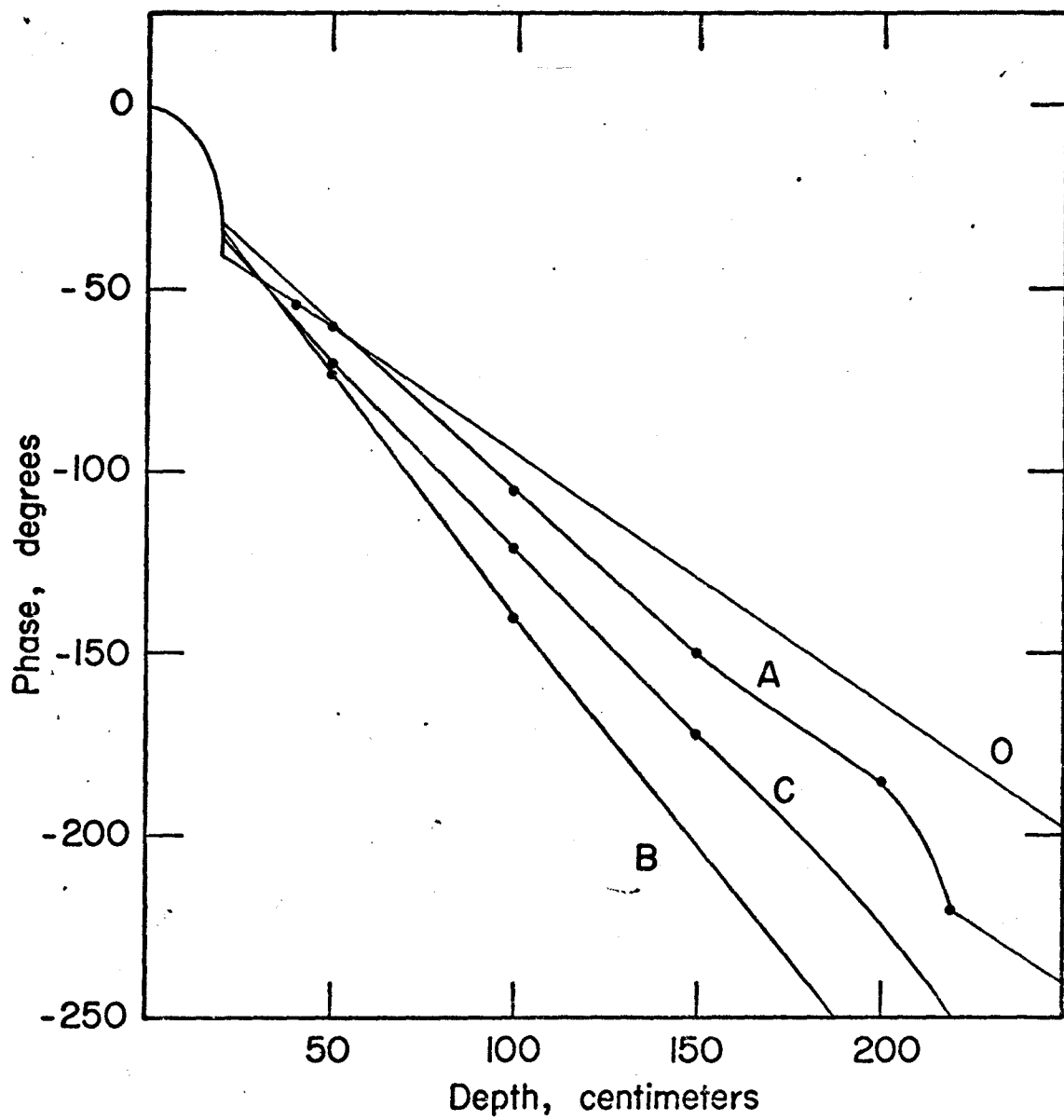


Figure 3 b. Phase lags in layers of figure 3 a.

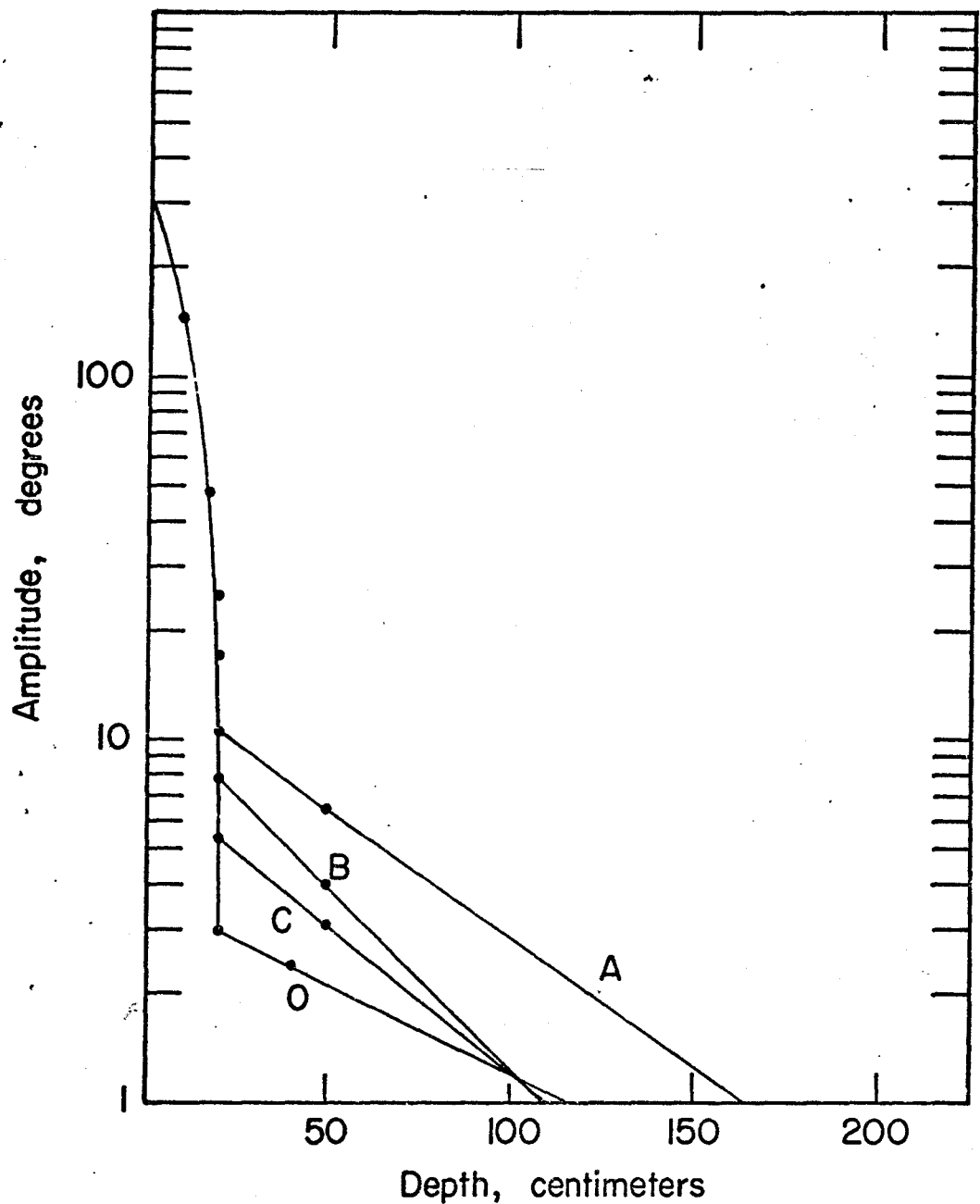


Figure 4 a. Effect of properties of the intermediate layer on amplitudes. Upper layer 20 cm. thick of material 3 of table 2 (I). Curves A, B, C for 200 cm of materials A, B, C of table 2 (II). Curve O, no intermediate layer, surface material rests directly on substratum.

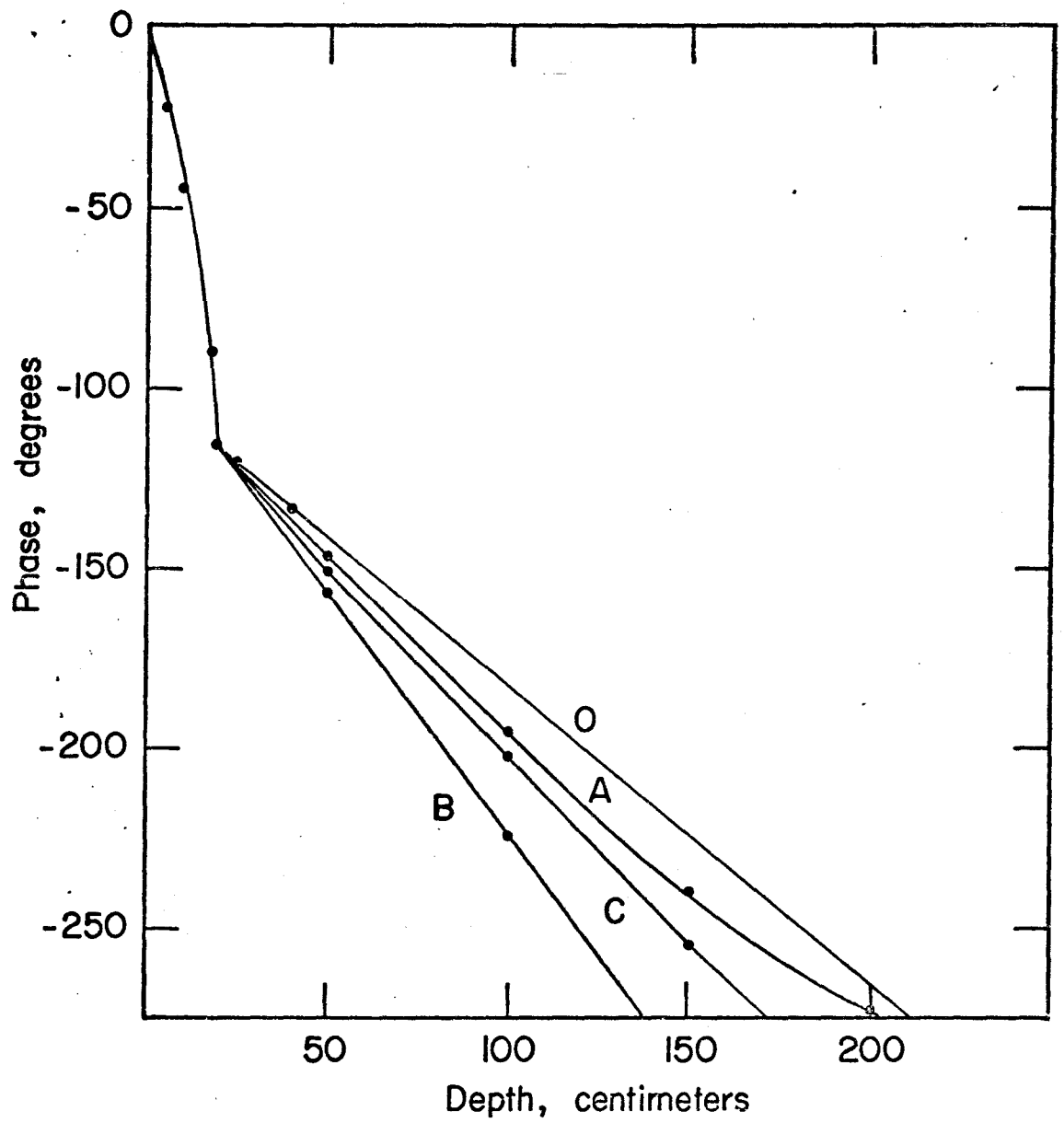


Figure 4 b. Phase lags in layers of figure 4 a.

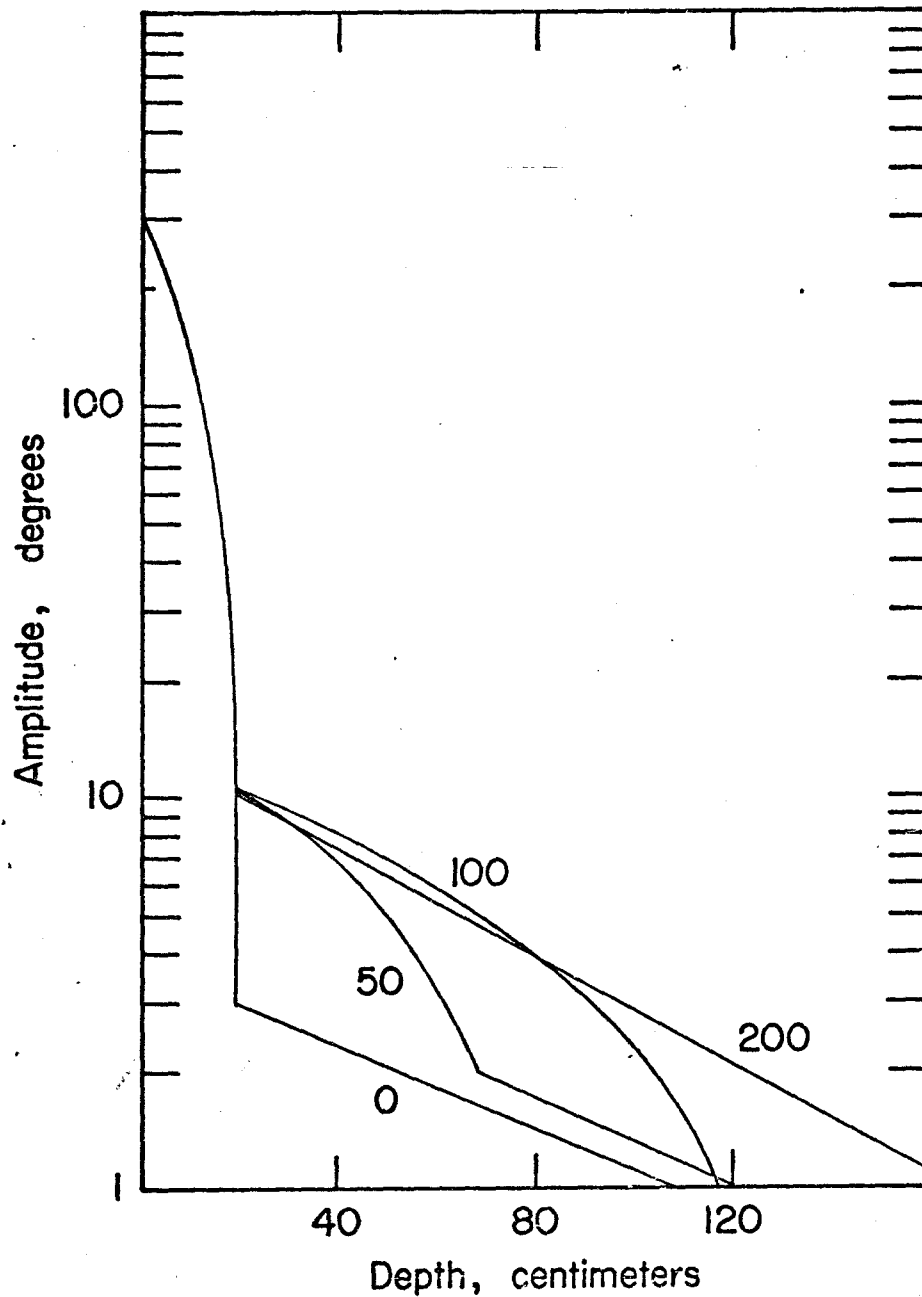


Figure 5. Effect of thickness of the intermediate layer on amplitudes. Upper layer 20 cm. thick of material 3 of table 2 (I), intermediate layer of material A of table 2 (II). Numbers beside curves give thickness of intermediate layer.

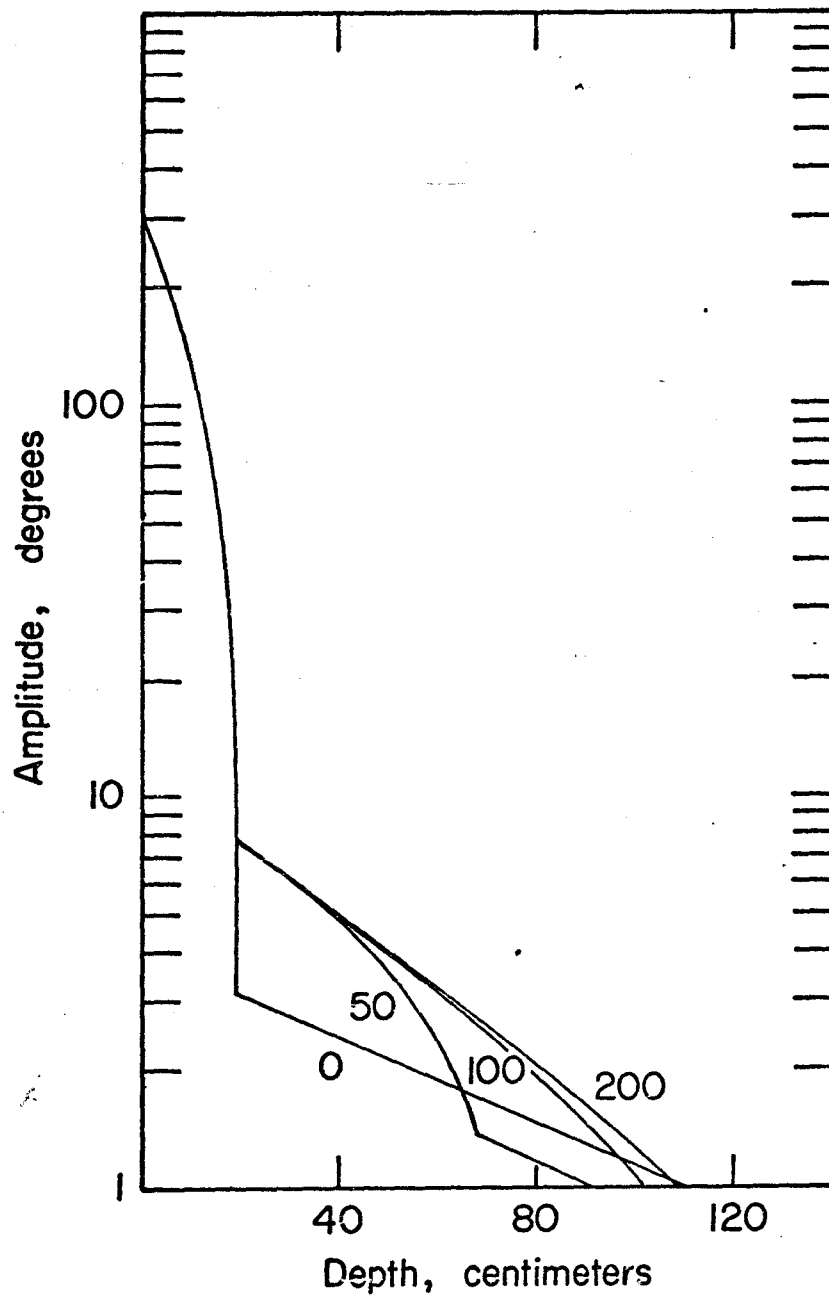


Figure 6. Effect of thickness of the intermediate layer on amplitudes. Upper layer 20 cm. thick of material 3 of table 2 (I), intermediate layer of material B of table 2 (II). Numbers beside curves give thickness of intermediate layer.

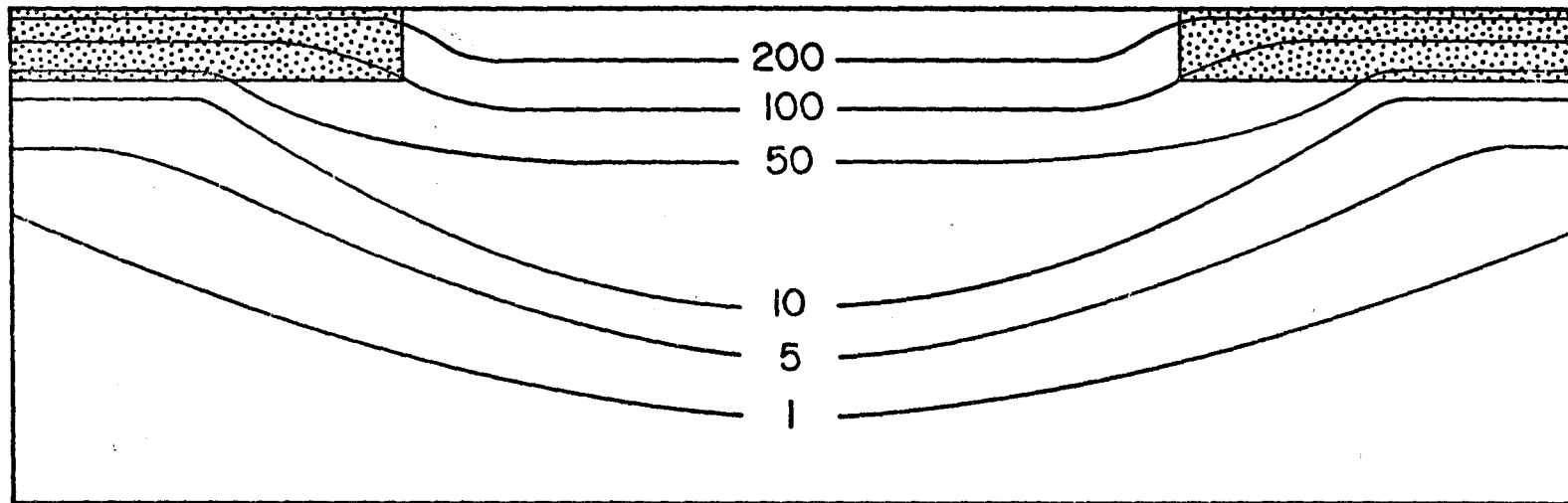
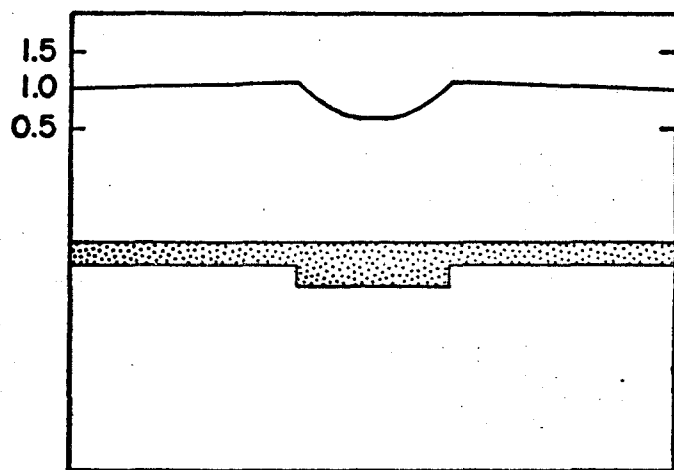
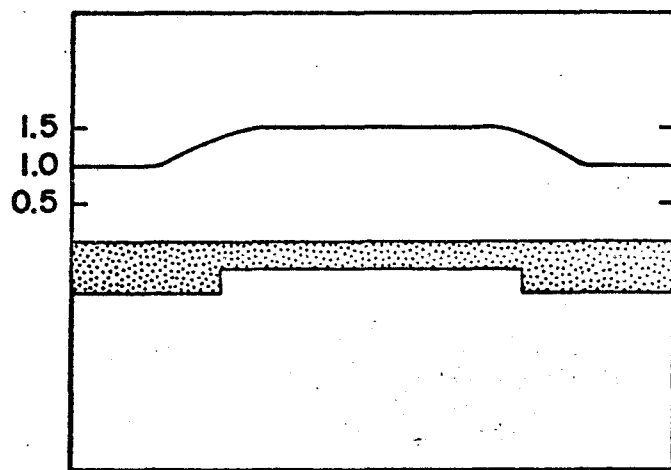


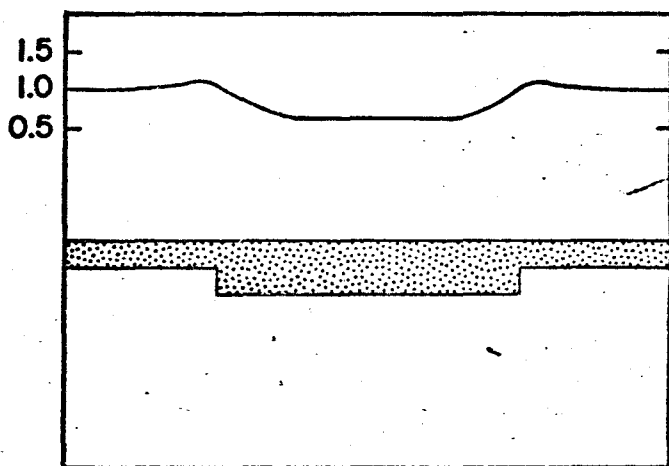
Figure 7. Amplitudes near a circular hole in the poorly conducting surface layer. Lines of constant amplitude are shown for a surface amplitude of 269°C , and a conductivity ratio of 10.



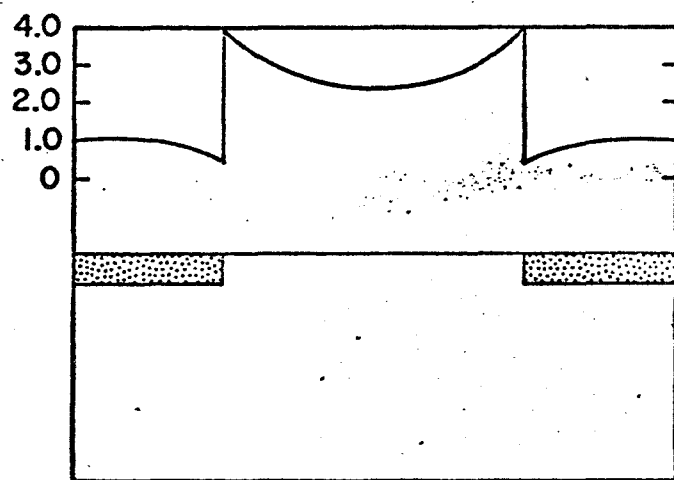
a



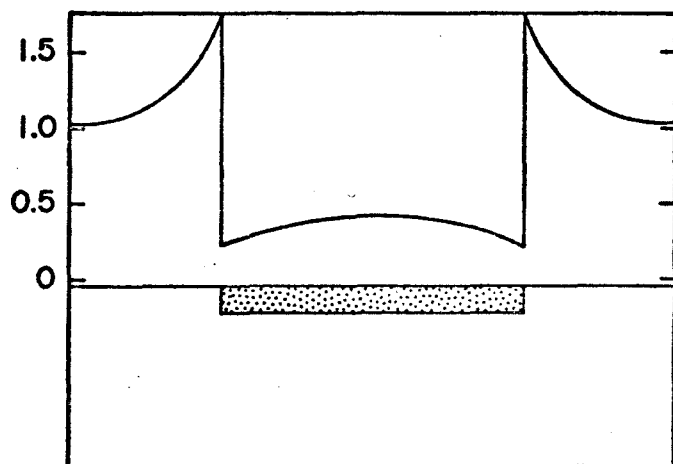
b



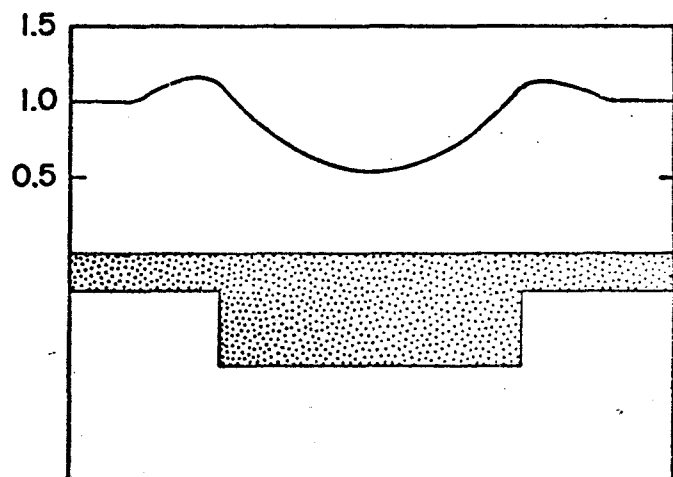
c



d



e



f

Figure 8. The effect of a number of configurations of the interface between the surface layer (stippled) and the substratum on heat flow. In all cases the protuberance has the shape of a right circular cylinder. The line at the top of each figure shows the ratio of flux at a given point to the flux at great distance from the irregularity for a conductivity contrast of 10. The configuration of layer is shown at the bottom of the figures.

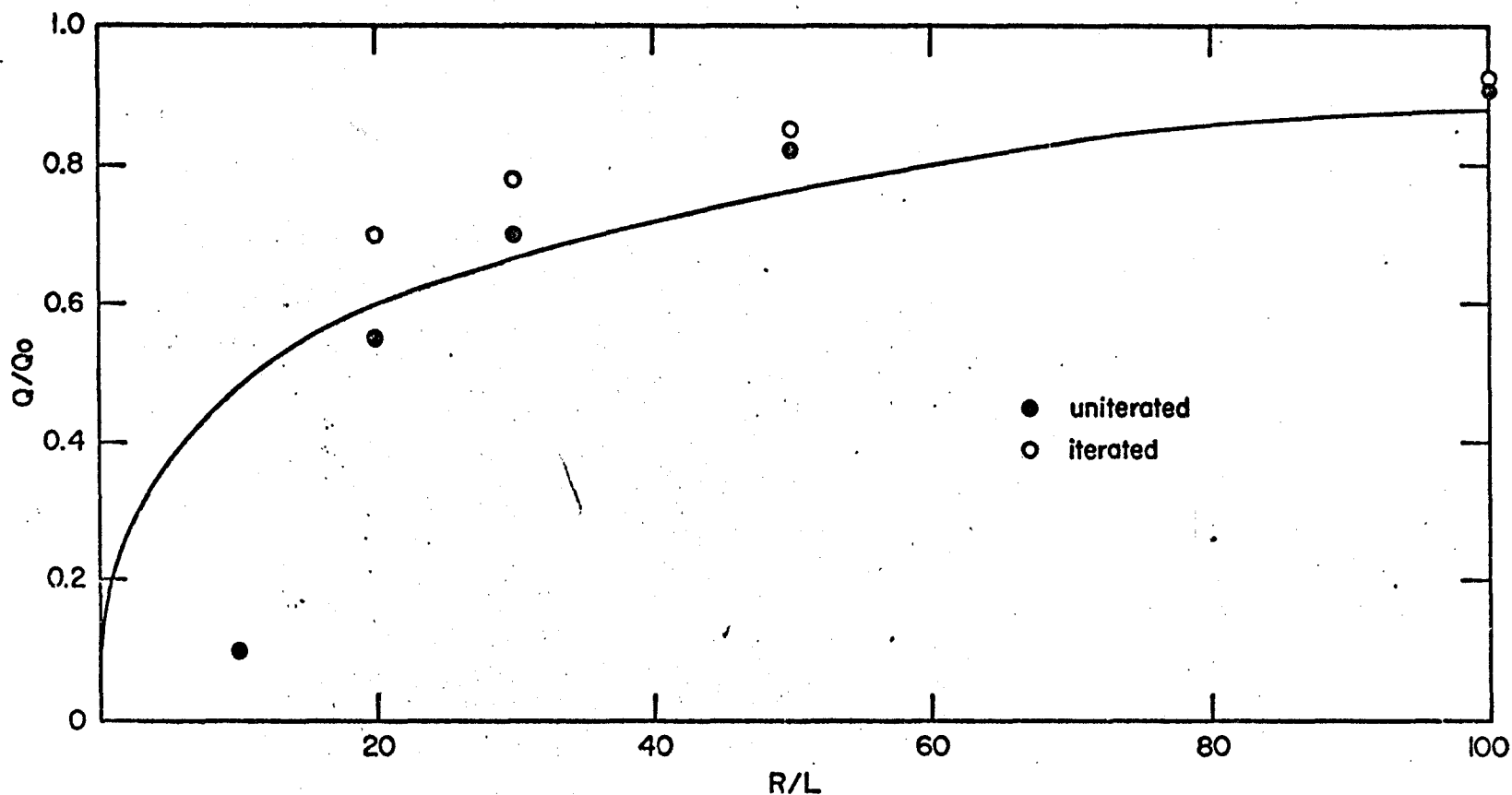


Figure 9. Comparison between the simple method of calculating the disturbance due to the blanket (equation 26) and the finite-difference calculation. The points were obtained from the equation with and without iterating the calculation and the line shows the finite-difference results.

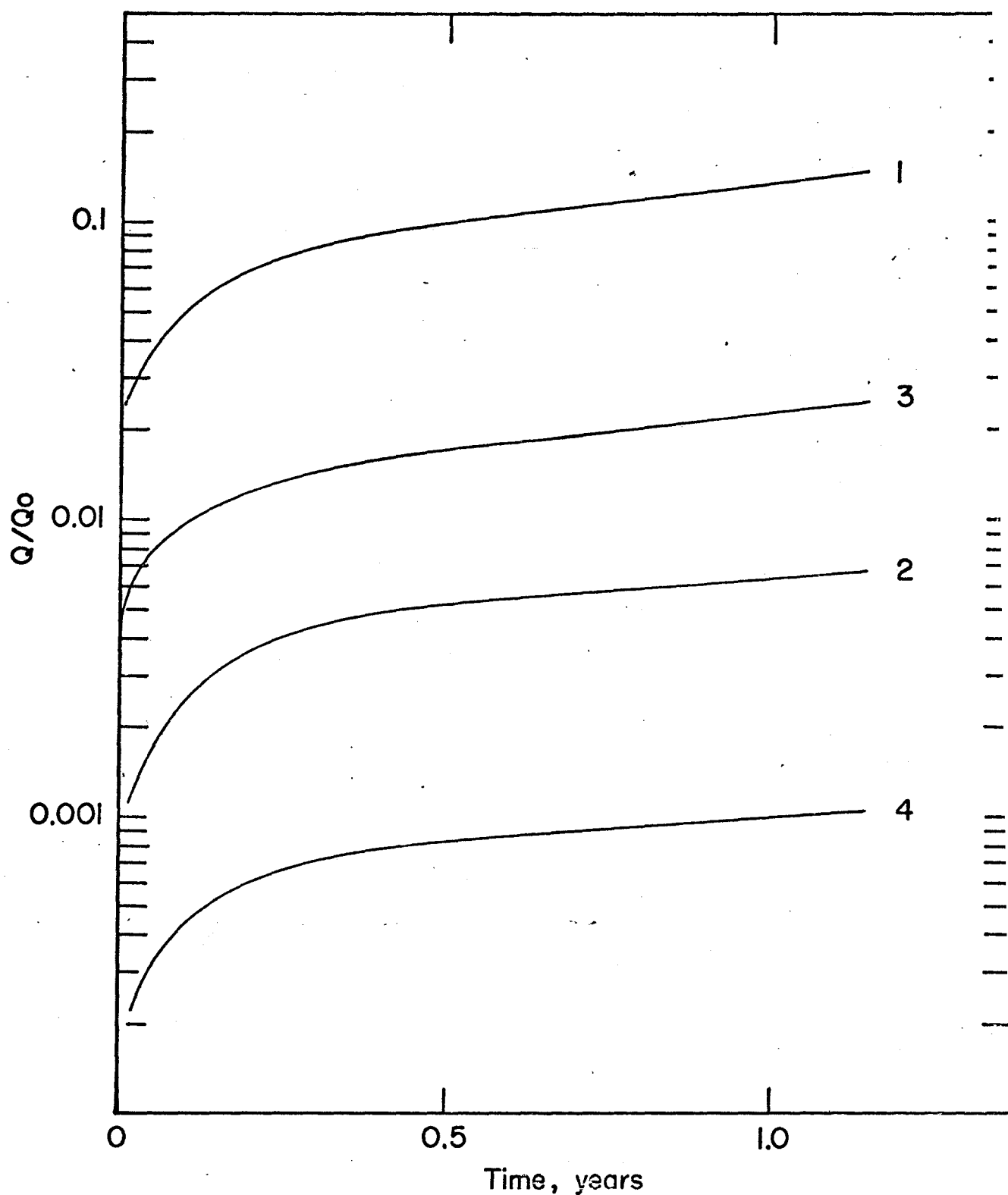


Figure 10. Ratio of transient to steady-state fluxes for times up to a year after blanket emplacement. Curves 1 and 2 for blanket of SI-10 material, curves 3 and 4 for SI-91 (table 2 (IV)). Curves 1 and 3 for blanket resting on dust (table 2 (I) 2), and curves 2 and 4 for blanket resting on substratum (table 2 (III)).

APPENDIX II

Numerical Simulation of the Conductivity Measurement

THE IN SITU MEASUREMENT OF LUNAR THERMAL CONDUCTIVITY

by Sydney P. Clark, Jr.

Interim Report

January 1967

Prepared under Grant No. NGR-07-004-039

Yale University

New Haven, Connecticut

The information presented herein was developed from NASA-funded work. Since the report preparation was not under NASA control, all responsibility for the material in this document must necessarily reside in the author.

NATIONAL AERONAUTICS AND SPACE ADMINISTRATION

Introduction

The measurement of heat flow at a lunar site requires knowledge of both the vertical thermal gradient and the local thermal conductivity. The former quantity can be measured more or less straight forwardly by a suitably instrumented probe emplaced in a drilled hole, but the latter presents special complications. In normal determinations of terrestrial heat flow, the conductivities of samples cored from the hole are measured in the laboratory. It is undesirable, and may even be impossible, to rely solely on this technique for lunar heat flow, since the sample may either be destroyed or may have its thermal properties seriously altered by the operations of collection and return to earth. Hence the determination of thermal conductivity in situ on the moon is clearly desirable and perhaps essential. This report deals with a preliminary study of a method of making this measurement which utilizes a cylindrical ring source. The results presented here form some of the fundamental criteria used in the design of a subsurface thermal probe for ALSEP by Arthur D. Little, Inc.

Theory

Consider a cylindrical hole of radius \underline{R} , infinite in length, containing a cylindrical probe, also of radius \underline{R} . Between $-\underline{Z}$ and \underline{Z} the probe consists of a heater of thermal conductivity \underline{k}_1 , density ρ_1 , and heat capacity \underline{c}_1 . For $|\underline{z}| > \underline{Z}$ the probe has thermal properties \underline{k}_2 , ρ_2 , and \underline{c}_2 , and there is no thermal resistance at $\underline{z} = \pm \underline{Z}$. The lunar material surrounding the hole has thermal properties \underline{k}_3 , ρ_3 , and \underline{c}_3 and there is contact resistance at $\underline{r} = \underline{R}$ such that a temperature drop $\Delta \underline{T}$ occurs, given by $\Delta \underline{T} = \frac{k_n \partial \underline{T}}{H \partial \underline{r}}$ (the so-called radiation boundary condition). \underline{k}_n would be \underline{k}_1 at the outer surface of the heater, \underline{k}_2 at the outer surface of the probe, and \underline{k}_3 at the

inner surface of the hole. The temperature is initially zero everywhere, and heat is supplied uniformly over the surface of the heater at rate Q for time $0 \leq t \leq t_0$. We must find the temperature as a function of r , z , and t .

The conditions set forth in the preceding paragraph completely specify a boundary value problem in heat conduction, but since they involve both radial and axial flow in a heterogeneous medium, they are intractable analytically. The problem was solved by finite differences in the following way. Consider intervals in space and time δr , δz , δt , and integers i , j , and k such that $z = j\delta z$, $t = k\delta t$, and $r = i\delta r$ for $i \leq I_1$ and $r = (i - 1)\delta r$ for $i \geq I_2 = I_1 + 1$. The temperature may be regarded as a function of i , j , and k . $I_1 \delta r = I_2 \delta r = R$, the radius of the hole. However $T(I_1, j, k) \neq T(I_2, j, k)$ because of the contact resistance, although the two points are only infinitesimally separated in space. On the other hand at $z = Z = J\delta z$, the temperature is continuous. Since the temperatures are symmetric about the axis of the cylinder and also about the plane $z = 0$, we need consider only positive values of r and z .

The equations used in the finite-difference calculation depend on the points at which the temperature is to be obtained. Referring to the schematic space grid shown in Figure 1, let $\alpha_1 = k_1/\rho_1 c_1$ be the thermal diffusivity in region 1, the heater, α_2 be the diffusivity in region 2, etc. Also, let $M_n^r = \alpha_n \delta t / \delta r^2$ and $M_n^z = \alpha_n \delta t / \delta z^2$, where $n = 1, 2, 3$. Then we have on the axis

$$T(0, j, k+1) = T(0, j, k) (1 - 4M_n^r - 2M_n^z) + T(1, j, k) \cdot 4M_n^r + [T(0, j+1, k) + T(0, j-1, k)]M_n^z \quad j \neq J, n = 1, 2, \quad (1)$$

$$\begin{aligned}
T(0, J, k+1) = & T(0, J, k) \left[1 - \left(4 \frac{\delta t}{\delta r^2} + 2 \frac{\delta t}{\delta z^2} \right) \left(\frac{k_1 + k_2}{\rho_1 c_1 + \rho_2 c_2} \right) \right] + T(1, J, k) \cdot \\
& \cdot 4 \frac{\delta t}{\delta r^2} \frac{k_1 + k_2}{\rho_1 c_1 + \rho_2 c_2} + T(0, J+1, k) \cdot 2 \frac{\delta t}{\delta z^2} \frac{k_2}{\rho_1 c_1 + \rho_2 c_2} + \\
& + T(0, J-1, k) \cdot 2 \frac{\delta t}{\delta z^2} \frac{k_1}{\rho_1 c_1 + \rho_2 c_2} \quad (2)
\end{aligned}$$

In the interiors of regions 1 and 2

$$\begin{aligned}
T(i, j, k+1) = & T(i, j, k) (1 - 2M_n^r - 2M_n^z) + [T(i, j+1, k) + T(i, j-1, k)]M_n^z \\
& + \left[\left(1 - \frac{1}{2i} \right) T(i-1, j, k) + \left(1 + \frac{1}{2i} \right) T(i+1, j, k) \right] M_n^r \quad (3) \\
& n = 1, 2, 0 < i < I_1, j \neq J.
\end{aligned}$$

and in region 3

$$\begin{aligned}
T(i, j, k+1) = & T(i, j, k) (1 - 2M_3^r - 2M_3^z) + [T(i, j+1, k) + T(i, j-1, k)]M_3^z \\
& + \left[\left(1 - \frac{1}{2i-2} \right) T(i-1, j, k) + \left(1 + \frac{1}{2i-2} \right) T(i+1, j, k) \right] M_3^r, \\
& i > I_2 \quad (4)
\end{aligned}$$

Along the outer skin of the heater and probe, we have, setting $f_n = \frac{2I_1 - 1}{I_1 - 1/4} M_n^r$

$$g_n = \frac{2I_1 H \delta t}{(I_1 - 1/4) \rho_n c_n \delta r},$$

$$\begin{aligned}
T(I_1, j, k+1) = & T(I_1, j, k) (1 - 2M_n^z - f_n - g_n) \\
& + [T(I_1, j-1, k) + T(I_1, j+1, k)]M_n^z \\
& + T(I_1 - 1, j, k)f_n + T(I_1 + 1, j, k)g_n, n = 1, 2, j \neq J \quad (5)
\end{aligned}$$

and

$$\begin{aligned}
 T(I_1, J, k+1) = & T(I_1, J, k) \left(1 - \frac{2(K_1 + K_2)\delta t}{(\rho_1 c_1 + \rho_2 c_2)\delta z^2} - \frac{2I_1 - 1}{I_1 - 1/4} \frac{K_1 + K_2}{\rho_1 c_1 + \rho_2 c_2} \frac{\delta t}{\delta r^2} \right. \\
 & - \frac{4I_1 h \delta t}{(I_1 - 1/4)(\rho_1 c_1 + \rho_2 c_2)\delta r} \left. \right) + T(I_1, J-1, k) \frac{2H_1 \delta t}{(\rho_1 c_1 + \rho_2 c_2)\delta z^2} \\
 & + T(I_1, J+1, k) \frac{2K_2 \delta t}{(\rho_1 c_1 + \rho_2 c_2)\delta z^2} \\
 & + T(I_1 - 1, J, k) \frac{2I_1 - 1}{I_1 - 1/4} \frac{1 + 2}{\rho_1 c_1 + \rho_2 c_2} \frac{\delta t}{\delta r^2} \\
 & + T(I_2, J, k) \frac{4I_1 H \delta t}{(I_1 - 1/4)(\rho_1 c_1 + \rho_2 c_2)\delta r} \quad (6)
 \end{aligned}$$

At times when the heater is on, terms accounting for its effect must be added to the right sides of (5) in region 1 and (6). We write

$$q = \frac{Q \delta t}{26.289 \delta r^2 \delta z J (I_1 - 1/4)}, \quad (7)$$

where the numerical factor includes the conversion from total power input, Q , in watts to the units of c.g.s. and calories in which the thermal properties were expressed. Then a term $q/\rho_1 c_1$ must be added in (5) and a term $q/(\rho_1 c_1 + \rho_2 c_2)$ must be added in (6) to account for the heat input.

Along the wall of the hole in the lunar material we have, setting

$$\underline{f}' = \frac{2I_1 + 1}{I_1 + 1/4} M_3^r \quad \text{and} \quad g' = \frac{2I_1 H \delta t}{(I_1 + 1/4)(\rho_3 c_3 \delta r)},$$

$$T(I_2, j, k+1) = T(I_2, j, k)(1 - 2M_3^Z - f' - g') + [T(I_2, j+1, k) + T(I_2, j-1, k)]M_3^Z + T(I_2+1, j, k)f + T(I_1, j, k)g \quad (8)$$

Finally, along the junction between the heater and the rest of the probe

$$\begin{aligned} T(i, J, k+1) = & T(i, J, k) \left[1 - \frac{2(K_1 + K_2)\delta t}{(\rho_1 c_1 + \rho_2 c_2)\delta r^2} - \frac{2(K_1 + K_2)\delta t}{(\rho_1 c_1 + \rho_2 c_2)\delta z^2} \right] \\ & + T(i, J+1, k) \frac{2K_2\delta t}{(\rho_1 c_1 + \rho_2 c_2)\delta z^2} + T(i, J-1, k) \frac{2K_1\delta t}{(\rho_1 c_1 + \rho_2 c_2)\delta z^2} \\ & + [T(i-1, J, k)(1 - \frac{1}{2i}) + T(i+1, J, k)(1 + \frac{1}{2i})] \\ & \frac{(K_1 + K_2)\delta t}{(\rho_1 c_1 + \rho_2 c_2)\delta r^2}, \quad 0 < i < I_1 \end{aligned} \quad (9)$$

Numerical stability proved to be a serious problem. In the interiors of the three regions, the stability criterion is

$$1 - 2M_n^Z - 2M_n^F > 0, \quad n = 1, 2, 3. \quad (10)$$

Depending on the relative thermal properties of probe, heater, and moon, a more stringent requirement may occur along the axis $i = 0$, since here the criterion is

$$1 - 2M_n^Z - 4M_n^F > 0, \quad n = 1, 2 \quad (11)$$

But even with (10) and (11) satisfied, instability, which always originated at $i = I_1$ and I_2 , was sometimes encountered, particularly for relatively large values of H . Imposing the additional constraints that

$$1 - 2M_n^Z - f_n - g_n > 0, \quad n = 1, 2$$

and

$$1 - 2M_3^2 - f' - g' > 0,$$

did not remove the difficulty. This instability may result from the fact that the space step δr is effectively halved at $i = I_1$ and I_2 , but the matter remains unresolved. The time step, δt , was simply reduced until the calculation became stable.

A second form of numerical difficulty, which may be termed semistability, was also encountered occasionally. Immediately after the heater was turned on or off, thus disturbing the system, the calculations oscillated, sometimes rather violently. The oscillations were damped, however, and the results gradually returned to a smooth trend with further cycles of iteration. This semistability could also be eliminated by reducing δt , thus approximating more closely a smooth input of heat.

Models

A number of models of probes and of the lunar material have been subjected to numerical analysis. The results are extensive and only the more relevant ones have been selected for inclusion here. Thermal properties of 3 of the probes are shown in Table 1. The thermal conductivity of Probe 1 is too low to be practical from an engineering standpoint, but the lunar probe is expected to have properties in the range of Probes 5 and 6. Further calculations will be necessary when the final configuration of the lunar probe is established and its properties are measured.

Table 1. Thermal characteristics of probes.

No.	0	1	5	6
Heater				
k, cal/cm sec°C	0	3×10^{-7}	10^{-4}	10^{-3}
ρ , gm/cm ³	—	4×10^{-2}	0.5	0.5
c, cal/gm°C	—	0.2	0.2	0.2
Probe body				
k, cal/cm sec°C	0	3×10^{-7}	10^{-4}	10^{-3}
ρ , gm/cm ³	—	4×10^{-2}	0.5	0.5
c, cal/gm°C	—	0.2	0.2	0.2

Moon models are shown in Table 2. Three different thermal conductivities differing by factors of 10 were used, and for the lower conductivities, densities, and hence diffusivities, differing by a factor of 4 were considered. These models cover the range of values considered likely for material close to the lunar surface. The ability of a probe to discriminate between them is then a measure of its suitability.

Table 2. Thermal models of moon.

No.	k, cal/cm sec°C	ρ , gm/cm ³	c, cal/gm°C
1	10^{-5}	0.5	0.2
2	10^{-5}	2.0	0.2
6	10^{-3}	1.6	0.2
7	10^{-4}	0.5	0.2
8	10^{-4}	2.0	0.2

Another parameter entering the calculations is the contact resistance, measured by the quantity \underline{H} . For purely radiative contact $H = 5.5 \times 10^{-12} \frac{E}{T^3}$, where E is the emissivity. With blackbody conditions $\underline{H} = 4.4 \times 10^{-5}$ at 200°K which is close to the mean lunar temperature. This is about the lowest value that \underline{H} can attain, and it is an interesting case to consider because the probe may be designed to assure purely radiative coupling. \underline{H} can then be calculated with confidence, whereas it otherwise remains an unknown parameter the value of which must somehow be extracted from the temperature-time curve. The effect of varying \underline{H} was examined by making some runs with it set at 10 times the radiative value.

The lunar probes are to be about 1.9 cm in diameter. The quantity δr was taken to be 0.475 cm, which places the probe skin at $i = 2$, and δz was taken equal to δr . This is a rather coarse grid, but no refinement of it was made in these preliminary studies. The simulation of a 14-hour lunar experiment required over 30 minutes on a 7094 in unfavorable cases, and it is not worthwhile to choose smaller space steps (which requires reduction of the time step as well to maintain stability) until more than hypothetical values of the probe parameters are available.

The length of the heater was taken equal to its diameter, 1.9 cm. In rough design calculations it may be desirable to approximate the probe configuration using the exact solution for radial flow from a spherical heat source, and the "square" shape chosen for the heater gives the closest possible approximation to a sphere. Thus the results of this work may be compared directly with those obtained from the spherical approximation. It should be noted that in the latter approximation no account of different thermal properties between the body of the probe and the lunar material can be taken.

Numerical results

It is helpful at the outset to consider the solution for an infinite cylindrical source of heat in an infinite medium. In this case the temperatures depend on the thermal conductivity and thermal diffusivity of the medium, and on the contact resistance. One could hope that the dependence on diffusivity could be removed by heating until the temperatures became steady, but with this geometry there is no steady state. The temperature of the source continues to rise indefinitely. With a heater of finite length a steady state is reached; this was an initial reason to prefer the geometry adopted here to the "line source" geometry, because the possibility exists of eliminating the diffusivity as a factor upon which the temperature depends. Another attractive feature of the present configuration is its relatively low power requirement. A line source demands a certain amount of power per unit length to produce a given temperature rise. Hence a long source requires high power. In the present case, it was found that 2 milliwatts input power gave adequate temperature rises at the heater, and this value for the heat input was used in all the calculations.

The first calculations were aimed at investigating the possibility of achieving a steady state. Results are shown in Figure 2. In this figure and those following, the temperatures are those of the outer surface of the probe. In actual lunar probes the temperature sensors will be located on the axis, but the temperature difference between these 2 points is insignificant for present purposes. It is clear from the figure that for the lower values of k the steady state is not achieved after 14 hours, and several days of heating may be required to attain it if k is less than 10^{-4} . If $k = 10^{-3}$ a few hours suffice. The probe is evidently

capable of discriminating between various values of \underline{K} , particularly if the heater is operated at low power levels for a long time. The discrimination is best at low \underline{K} , and heating should last for the order of a day or more for optimum results.

Similar curves for the case of $1/10$ as much contact resistance are shown in Figure 3. The discrimination is somewhat better than in Figure 2, and the curves have a different shape. The sharp initial rise in temperature is much reduced. In Figure 4 the results for a probe of higher conductivity are shown; the discrimination is not as good as in Figure 2. Clearly the thermal conductivity of the probe should be kept as low as possible.

These results show that it is likely that the temperature rise recorded during the lunar experiment will depend on the 3 quantities \underline{K} , α , and \underline{H} . Some process of curve fitting must be used to determine their values. This may be unsatisfactory since many combinations of parameters may give virtually identical results. It is therefore important to try to extract more information from the experiment, and an obvious way to do this is to record the temperatures at more than one point along the probe. The temperature rise at a point on the surface of the probe 8 cm from the center of the heater is shown in Figures 5 and 6. Figure 5 is for a probe of unrealistically low \underline{K} , but it shows the large differences in rise time that result from the different moon models. Intuitively one would expect the curves to be highly sensitive to α and this is born out by the difference between curves 1 and 2 of Figure 6. The rise times are about the same for the cases shown there, in which the conductivity of the probe is realistic. But if the moon is a better conductor than the probe discrimination still exists at short times, although it is not well-shown on a plot to the scale of Figure 6. Since this is just the

range of conductivity at which the temperatures at the center of the heater lose discrimination, complementary information can be obtained from the second sensor.

So far we have confined the discussion to times when the heater was turned on. But a number of short-term numerical experiments have been done in which the heater was turned on for only half the time. The durations of the tests were about $\frac{1}{2}$ hour. The results were that the appearances of the cooling curves were virtually identical to the heating curves, but of course inverted and displaced in time. Thus there is no new information to be obtained from the cooling curves. On the other hand, following the cooling curve in effect constitutes repeating the heating experiment, but without the necessity of expending heater power. It is always desirable to repeat experiments if only to get better statistical control.

Operations on the moon

All lunar experiments must wait until drilling disturbances have died out near the hole. The thermal gradient will be determined next and then the heater will be turned on at low power (~ 2 milliwatts). The duration of the heating cycle will be determined by the conductivity encountered. The heater will then be turned off and the cooling curve followed until ambient conditions have essentially reestablished themselves. Then, especially if a high lunar thermal conductivity is indicated by this experiment, a second heating period will be initiated. The heater power will be higher (20 milliwatts or more) so that the second sensor, displaced along the probe from the heater, will record a readily measured temperature rise. By a process of curve fitting, which is not completely thought out as yet, the quantities K , α , and H will be determined. The first 2 of these automatically yield a value of ρc , which

can be compared with the value measured on returned material to give a rough check on the internal consistency of the results. An alternative scheme would be to assure that H is known independently e.g. by making certain of radiative coupling alone; then only k and α need be obtained from the temperature curves and the accuracy of the measurements will be increased.

Conclusions

1. It appears feasible to measure lunar thermal conductivity using a cylindrical ring source of heat.
2. It is desirable to have 2 heating cycles, the first at a power level of a few milliwatts and the second at 10 or more times that power.
3. The duration of each heating will range from a few hours to a few days, depending on the lunar conductivity. The use of 2 sensors and 2 power levels could materially reduce the amount of heating time required.
4. There is something to be said for assuring radiative coupling to the moon so that the contact resistance can be calculated with confidence. Otherwise it represents a third unknown parameter to be determined from the temperature curves. Some discrimination of lunar conductivity is lost by this procedure, but nevertheless more accurate results will probably be obtained.
5. The best way of reducing the lunar data remains to be determined.